REPORT NO. 52

February, 1952

THE COLLEGE OF AERONAUTICS

CRANFIELD

The Distribution of Pressure over the Surface of Wings of Small Aspect Ratio*

-by-

W.S.D. Marshall, D.Ae.(Hull), A.F.R.Ae.S.

SUMMARY

The distributions of pressure over wings of aspect ratio 1.5 and 0.5 have been measured for a range of incidence up to and including the stall at various angles of yaw. This report presents a detailed analysis of the results at two incidences corresponding to 1/4 and 3/4 of the stalling incidences approximately. Direct measurements of lift and pitching moment have also been made, and the results compared with the results of theory and previous experiments.

The analysis shows that.-

1. Regions of high suctions near the tips assume greater importance as the aspect ratio is reduced. This tip suction rapidly increases in intensity with increase in incidence.

2. Apart from regions near the tips the spanwise distribution of load becomes more nearly elliptical with decrease in aspect ratio.

3. The effect of a positive sideslip is to skew the spanwise load grading curve and to produce a negative rolling moment. This effect is more pronounced at small aspect ratios.

/4. ...

MEP

---

* Much of the experimental work, upon which this note is based, was performed by Messrs. E.G. Havard, E.F. Lawlor, A.Lightbody, and A.O. Ormerod in 1948.

4. Comparison between the lift coefficients obtained by direct measurement and from the pressure distributions shows reasonable agreement and the variations of lift curve slope with change in aspect ratio are in agreement with the results of other workers.[1,7] Further, a theoretical curve due to Wieghardt[8] shows close agreement with the present experimental values.

5. The method developed by Flax and Lawrence,[2] based on a modified slender body theory, for estimating the position of the aerodynamic centre is found to be in reasonable agreement with the experimental results.

LIST OF CONTENTS

		Page No.
1.0	Introduction	4
2.0	Details of tests	4
3.0	Results	5
4.0	Discussion	7
	4.1. The Distribution of Pressure	7
	4.2. Spanwise Load Grading	8
	4.3. Tip Effects	8
	4.4. Spanwise Variation in Position of local Centre of Pressure	9
	4.5. Aerodynamic Derivatives	9
	4.5.1. Normal Force with Respect to Sideslip	9
	4.5.2. Pitching Moment due to Sideslip	9
	4.5.3. Rolling Moment due to Sideslip	10
	4.6. Direct Measurements of Lift and Pitching Moment	10
	4.6.1. The Lift Curves	10
	4.6.2. Pitching Moment Results	11
5.0	Conclusions	11
	List of References	12
	Table I - Ordinates of the Aerofoil Profile.	13

1.0 Introduction

Recent developments have stimulated interest in the characteristics of wings of small aspect ratio. The tests described here were concerned with the pressure distributions, normal force coefficients and the effects of yaw on wings of aspect ratio 0.5 and 1.5. The wings in this instance were rectangular with constant symmetrical sections 12 per cent thick. From the pressure distributions the spanwise loading and the positions of the local centres of pressure have been determined as well as the derivatives of the normal force, pitching and rolling moments with rate of yaw.

The pressure distribution measurements were made in the No. 2 Wind Tunnel at the College of Aeronautics during June and July of 1948, and later a few balance measurements of lift and pitching moments were made in the No. 1A Wind Tunnel.

During the preparation of this report, the results of some Swedish experiments[1] came to hand. The work described in this reference covers much the same ground as the present experiments, and, where possible, comparison between the two sets of results is made.

2.0 Details of Tests

The models were made of laminated mahogany having the symmetrical section shown in Fig. 1. (The ordinates are given in Table I). The wing tips were half bodies of revolution. The chord of both wings was 15 in. and the spans were $22\frac{1}{2}$in and $7\frac{1}{2}$in., exclusive of wing tip fairings. The values of aspect ratio quoted apply strictly to the wings without tip fairings, the effective additional area and span due to the tip fairings having been neglected. The models were mounted from an overhead turntable by a combination of struts and wires, the arrangement of which can be seen in Figs. 2a and 2b.

Small bore tubes of a pliable plastic material were inlaid into chordwise slots cut in the top and bottom surfaces of the wing from the leading edge of the wing back to 85 per cent of the chord. The tubes were faired over with beeswax, and the model french polished. The upper surface tubes extended around the nose of the aerofoil and back along the lower surface to about 20 per cent of the chord. Lengths of rubber tubing transmitted the pressures to a vertical multitube manometer.

/The ...

The pressure orifices were formed by drilling holes in the tubes at a single chordwise position, and when the pressures at this position had been recorded these holes were sealed with plasticene and a fresh set of holes drilled at a different chordwise station.

The chordwise positions of the orifices were as follows.-

Upper Surface x/c	0, .01, .03, .05, .07, .10, .15, .25, .35, .45, .55, .65, .75, .85.
Lower Surface x/c	.02, .05, .10, .15, .25, .35, .45, .55, .65, .75, .85.

The tunnel speed for all tests was 120 ft./sec., corresponding to a Reynolds number of 0.95×10^6, and readings of pressure were taken at the following incidences (uncorrected).

Aspect Ratio 1.5	0°	5°	10°	15°	20°	22° (stalled)
Aspect Ratio 0.5	0°	6°	18°	25°	28° (stalled)	

The angles of sideslip, denoted by ψ, were 0°, 10° and 20° to starboard for both wings.

For the second series of tests each wing was suspended from the three component balance of the No. 1A tunnel and measurements of lift and pitching moment were taken over a range of nominal incidence from -4° to 10°.

3.0. Results

The pressure coefficients were plotted against chordwise positions for each of the wing attitudes tested, and smooth curves were drawn through the experimental points. A selection of the resulting isobars is given in figs. 3 - 14.

The area enclosed by the curves giving the upper and lower surface pressure distributions along the chord for any given spanwise position represents the normal force per unit span acting on the aerofoil at that spanwise position. That is, the local normal force coefficient, c_{NF} is given by

$$c_{NF} = \int_{x/c = 0}^{x/c = 1.0} (C_{p_{upper}} - C_{p_{lower}}) \, d\left(\frac{x}{c}\right).$$

/where ...

where x is the distance aft of the leading edge measured along the chord line.

On the wing of larger aspect ratio the lower surface pressures aft of the quarter chord point could not be measured at two of the spanwise positions, because the pressure holes would have been in the wake of the supporting struts. As there are no steep pressure gradients in this region, it was thought that little accuracy would be lost if the pressures there were obtained by interpolation from the pressures measured at the adjacent stations.

In the analysis it was necessary to draw complete spanwise load grading curves to obtain the total normal force coefficient acting on the wing. This involved a certain amount of extrapolation across the wing tip fairings. Since the normal force per unit span may be expected to be continuous and to reduce to zero at the tips this was the quantity extrapolated. Normal force per unit span can be represented by the non-dimensional coefficient $c_{NF} \times \frac{c}{c_{\mathbb{C}}}$. This coefficient has been plotted as the ordinate of the spanwise load grading curves in figs. 16 and 17. Over the parallel portion of the wing $c = c_{\mathbb{C}}$, so that an ordinate in this portion is simply the local normal force coefficient. In figs. 16 and 17 the curves are shown slotted where the extrapolation is doubtful.

The local centre of pressure was found as the point on the chord line through which, for the section considered, the resultant normal force acts. The position of this point was found graphically from the chordwise pressure distribution. The variations of the local centre of pressure are shown plotted in figs. 18 and 19.

By integrating the spanwise load grading curves the variation of normal force with angle of sideslip was obtained; and the variations of pitching and rolling moments with yaw were obtained by integration of curves giving the moments of the normal forces about the leading edge and the centre line respectively. The results are shown in figs. 20a,b and c.

The main correction due to tunnel constraint is a change in the measured angle of incidence at a constant wing lift coefficient. This correction has been applied to the readings although some doubts exist as to its validity on account of the large ratio of wing chord to tunnel diameter encountered in these tests. It is for this reason that, where possible, the overall normal force coefficient has been used as a parameter in the

/presentation ...

presentation of the results in preference to the angle of incidence.

4.0 Discussion

4.1. The Distribution of Pressure

The distributions of pressure over the wings are shown by lines of constant pressure coefficient (C_p) for the upper and lower surfaces in figs. 3 - 14. A striking feature shown by these isobars for the larger incidences is the high suctions occurring at the tips, near the trailing edge on the upper surface and, to a lesser extent, at about the mid-chord position on the lower surface. This phenomenon has been noted by other workers [1,2] and has been attributed to a spiral motion of the air from bottom to top surface around the tip fairings related to the component of flow normal to the plane of the wing.[2] This spiral motion is said to result in a trailing vortex springing from the wing surface which is separate in character, but which may become indistinguishable from the normal trailing vortices of lifting line theory. Certainly, tuft observations reveal marked cross flows of the type described, but the lift distribution and the associated vortex flow are related effects resulting from some more fundamental cause, which must be sought by further and more detailed investigations of the character of the boundary layer flow in the region of a wing tip.

Yawing the wing intensifies or diminishes these regions of suction according to whether the spanwise component of the flow due to yaw reinforces or opposes the inflow or outflow. This effect is clearly shown for $\gamma = 20^\circ$ (figs. 8 and 14), where the region of higher suction is confined to the leading tip on the upper surface and to the trailing tip on the lower surface.

In the case of both aspect ratios tested the regions of higher suction occurring on the top surfaces extend inboard of the tips for a distance approximately 15 per cent of the chord and it can be inferred that they are roughly of the same order of intensity at the same overall normal force coefficient. This is consistent with the hypothesis that the tip effect is not a characteristic solely of small aspect ratio wings and indeed something similar has been found[3] to occur on a wing of aspect ratio 6. On this hypothesis, the intensity and extent, expressed as a fraction of the wing chord, of the higher suction at the tips are approximately independent of aspect ratio but, as the aspect ratio decreases, these tip effects become relatively more important,

/since ...

since they extend over a larger fraction of the wing surface.

As already noted the wings tested were rounded at the tips by a surface obtained by revolving the aerofoil profile about a streamwise axis through the tip. This method of rounding produced a wing span which increased with distance from the leading edge up to the location of maximum thickness of the section (in this case at 0.3 of the chord) and then decreased to the leading edge span at the trailing edge. According to Jones,(4) for thin wings of very low aspect ratio, the lift is zero over the entire portion of the wing over which the span is decreasing if the trailing edge is sharp there and the Kutta-Joukowski condition applies. With the tips rounded as in these experiments the Kutta-Joukowski condition is not applicable there, but then the simple slender body theory, on which Jones' theory is based, predicts negative contributions to the lift where the span is decreasing. This is in agreement with more exact theories,(5) which predict small or negative lifts in that region. Inspection of the isobars given in figs. 4 and 10 and the spanwise pressure distributions of fig. 15 shows that the present experimental results support this prediction; it will be seen that the suction at the tips is more or less cancelled out by the region of pressure over the central part of the span towards the trailing edge.

4.2. Spanwise Load Grading (figs. 16 and 17)

Apart from the tip effects the loading distributions show an increasing tendency towards the elliptical distribution with reduction of aspect ratio, in agreement with theory.(4) As remarked above, however, the tip effects become more dominant with decrease of aspect ratio. The curves for both $\gamma = 10^{\circ}$ and 20° show that yaw tends to skew the load grading so that the lift is increased at the leading tip.

4.3. Tip Effects

At zero yaw and particularly at the large incidence the high suction region on the upper surface near the tips results in a local maximum or peak in the load grading curve. Holme(1) also noted this effect. With the wing yawed this peaking is more pronounced at the leading tip, whilst at the trailing tip it tends to disappear. These changes in loading at the tips are far more marked at high than at low incidences.

/4.4. ...

4.4. Spanwise Variation in Position of Local Centre of Pressure (Figs. 18 and 19)

The method of estimating centres of pressure is less accurate than that of estimating the normal force coefficient, C_{NF}, because.-

a) frictional drag effects were neglected

and b) pressures near the trailing edge were obtained by extrapolation, the rearmost reading of pressure having been made at 0.85 of the chord. These pressures have no little bearing on the centre of pressure position.

Nevertheless, the overall trends revealed by the data are of interest.

It appears that at zero yaw and small angles of incidence the centre of pressure tends to move forward as the tip is approached. With increase in incidence, however, the suction at the tips near the trailing edge results in a rapid rearward movement of the local centre of pressure there. It will be noticed that the curve for aspect ratio 0.5, $C_{NF} = 0.11$, $\psi = 0^{\circ}$ lacks symmetry, this lack of symmetry is a measure of the reliability of the deduced positions of the local centres of pressure in an extreme case where the accuracy can be expected to be least.

With increase in the angle of yaw, the centre of pressure on the leading tip moves back, and moves forward on the trailing tip. In general, it can be seen that the centre of pressure moves rearward with increase in incidence.

4.5. Aerodynamic Derivatives (Fig. 20)

4.5.1. Normal Force with Respect to Sideslip (z_v) (Fig. 20A)

For both aspect ratios the normal force coefficient C_{NF} remains constant with change of yaw at the smaller incidence. At the larger incidence there is a slight increase in C_{NF} with yaw.

4.5.2. Pitching Moment due to Sideslip (m_v) (Fig. 20B)

The method for estimating m_v from the pressure distributions is less accurate than that for ℓ_v and z_v, since, in this case, an accurate determination depends on an intimate

/knowledge ...

knowledge of the spanwise pressure distribution near the tips.

The results indicate that the pitching moment coefficient C_m becomes less negative for the smaller values of yaw and increases again with further increase in the angle of yaw. This may be attributed to the fact that for small angles of yaw the rate of build up of suction at the leading tip is less than the corresponding rate of decrease at the trailing tip. At the larger angles of yaw, however, this effect is reversed.

4.5.3. Rolling Moment due to Sideslip (l_v) (Fig.20C)

The skewing of the spanwise load grading curves produced by the sideslip causes a considerable rolling moment. The rolling moment derivatives obtained in the present experiment are compared in the following table with a semi-empirical law quoted by Levacic[6], based, however, on data relating to wings of larger aspect ratio than those considered here.

Nominal Aspect Ratio	1.5	0.5
High Incidence - l_v/C_{NF}	0.25	0.40
Low Incidence - l_v/C_{NF}	0.10	0.46
Levacic (ref. 6)	0.25	0.72

Some measure of agreement is obtained with Levacic's formula for the wings of higher aspect ratio, but for the smaller aspect ratio his formula considerably over-estimates l_v.

4.6. Direct Measurement of Lift and Pitching Moment

4.6.1. The Lift Curves

Fig. 21 shows the lift coefficient obtained by balance measurement plotted against incidence corrected for the effect of tunnel constraint. Also shown in fig. 2 are the results obtained from the pressure distributions. The agreement is thought to be satisfactory, bearing in mind that some extrapolation was necessary in determining the normal force coefficients.

The variation in lift curve slope at zero incidence with change in aspect ratio is shown in fig. 22. The results of

/this ...

this experiment show fair agreement with those of other workers.[1,7] Calculations[2,8,9] of this variation with aspect ratio based on different theories are also shown in fig. 22, and it is seen that the three curves are almost identical. If choice must be made, the curve due to Wieghardt (ref. 8), which assumes an elliptical load distribution, would seem to offer the best agreement with the present experimental values.

4.6.2. Pitching Moment Results

These results are presented in fig. 23 in the form of $C_m - C_L$ curves. For the balance measurements pitching moments were measured about an axis through the quarter chord point. The position of the aerodynamic centre has been determined by measurement of the slope of the curves at $C_L = 0$.

Fig. 24 shows a curve derived by the method of Flax and Lawrence (ref. 2) based on a slender body theory, where, however, the tips are considered separately from the rectangular portions of the wings, and the resulting loadings are added. The agreement between this curve and the measured results is satisfactory.

5. Conclusions

The main conclusions can be summarised as follows.-

a) Tip effects in the form of regions of high suctions on the upper surface near the trailing edge and on the lower surface near the mid chord position become relatively more important as the aspect ratio is reduced. The upper surface suction region rapidly increases in intensity as the incidence is increased.

b) Apart from regions near the tips, the spanwise distribution of load becomes more nearly elliptical as the aspect ratio is decreased.

c) The effect of sideslip is to skew the spanwise load grading curve so that a positive sideslip produces a negative rolling moment. The region of high suction on the upper surface at the tip becomes intensified by yaw, whilst that at the trailing tip becomes reduced. The effects are more pronounced with reduction in aspect ratio.

d) Comparison between the lift coefficients obtained by

/direct ...

direct measurement and from the pressure distributions shows reasonable agreement, and the variations of lift curve slope with change in aspect ratio are in agreement with the results of other workers.[1,7] Further, a theoretical curve for this variation due to Wieghardt[8] shows close agreement with the present experimental values.

e) The method developed by Flax and Lawrence,[2] based on a modified slender body theory, for estimating the position of the aerodynamic centre is found to be in reasonable agreement with the experimental results.

LIST OF REFERENCES

No.	Author	Title, etc.
1.	Holme, Olaf A.M.	Measurements of the Pressure Distribution on Rectangular Wings of Different Aspect Ratio. F.F.A. Report No. 37, 1950
2.	Flax, A.H. and Lawrence, H.R.	The Aerodynamics of Low Aspect Ratio Wings and Wing Body Combinations. Third Anglo-American Conference, 1951
3.	Knight, M. and Loeser, O.	Pressure Distribution over a Rectangular Monoplane Wing Model up to 90° Angle of Attack. N.A.C.A. Report No. 288. 1929
4.	Jones, R.T.	Properties of Low Aspect Ratio Pointed Wings at Speeds Below and Above the Speed of Sound. N.A.C.A. Report No. 835. 1946
5.	Lawrence, H.R.	The Lift Distribution on Low Aspect Ratio Wingsat Subsonic Speeds. I.A.S. Preprint No. 313. January, 1951
6.	Levacic, I.	Rolling Moment due to Sideslip, Part II. The Effect of Sweepback and Planform. R.A.E. Report No. Aero. 2092.Nov. 1945
7.	Scholz, N.	Kraft-und Druchverteilungsmessen an Tragflachen kleiner Streckung. Forschung auf dem Gebeite des Ingenieurwessens, Part B, Vol.16 No. 3, pp. 85-91. 1949-50
8.	Wieghardt, K.	Chordwise Load Distribution of a Simple Rectangular Wing. N.A.C.A. Tech.Memo No.963. Oct. 1940
9.	Weissinger, J.	The Lift Distribution of Sweptback Wings. N.A.C.A. Tech.Mem. No. 1120. 1947.

TABLE I

Ordinates of the Aerofoil Profile

x/c	± y/c
0	0
.013	.018
.025	.024
.050	.033
.075	.040
.100	.045
.150	.051
.200	.057
.250	.059
.300	.060
.350	.059
.400	.058

x/c	± y/c
.450	.055
.500	.051
.550	.047
.600	.042
.650	.038
.700	.032
.750	.027
.800	.022
.850	.016
.900	.011
.950	.006
1.000	.002

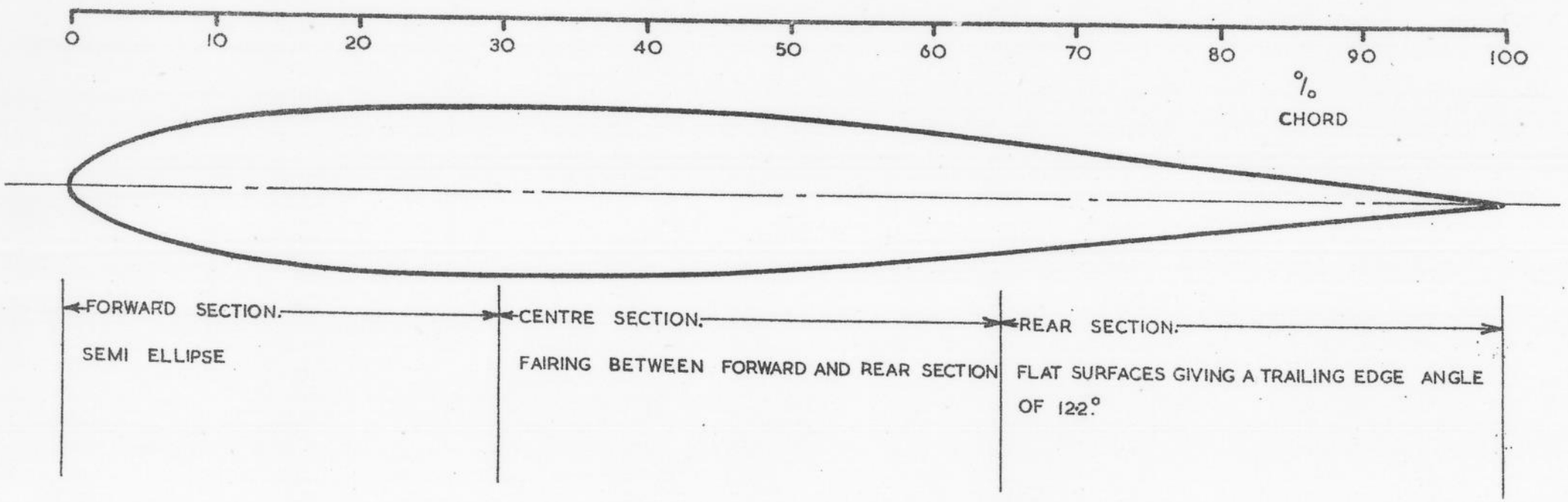

SYMMETRICAL SECTION, MAXIMUM THICKNESS CHORD RATIO = ·12, AT ·3c FROM THE LEADING EDGE.

DETAILS OF THE WING SECTION USED.

FIG. 1.

FIG. 2.A.&2.B.

FIG 2.B.

WING OF ASPECT RATIO ·5

FIG 2.A.

WING OF ASPECT RATIO 1·5

COLLEGE OF AERONAUTICS

REPORT No. 52.

FIG. 3.

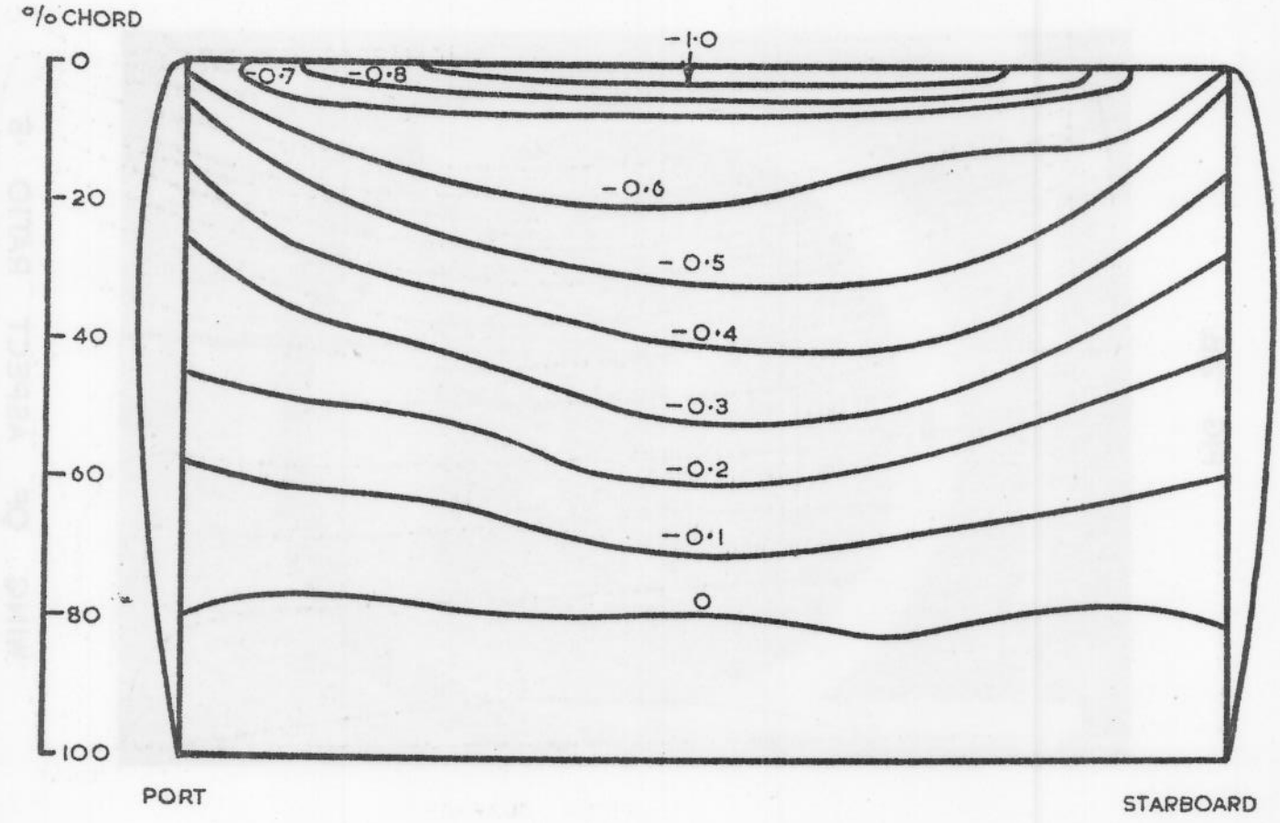

UPPER SURFACE

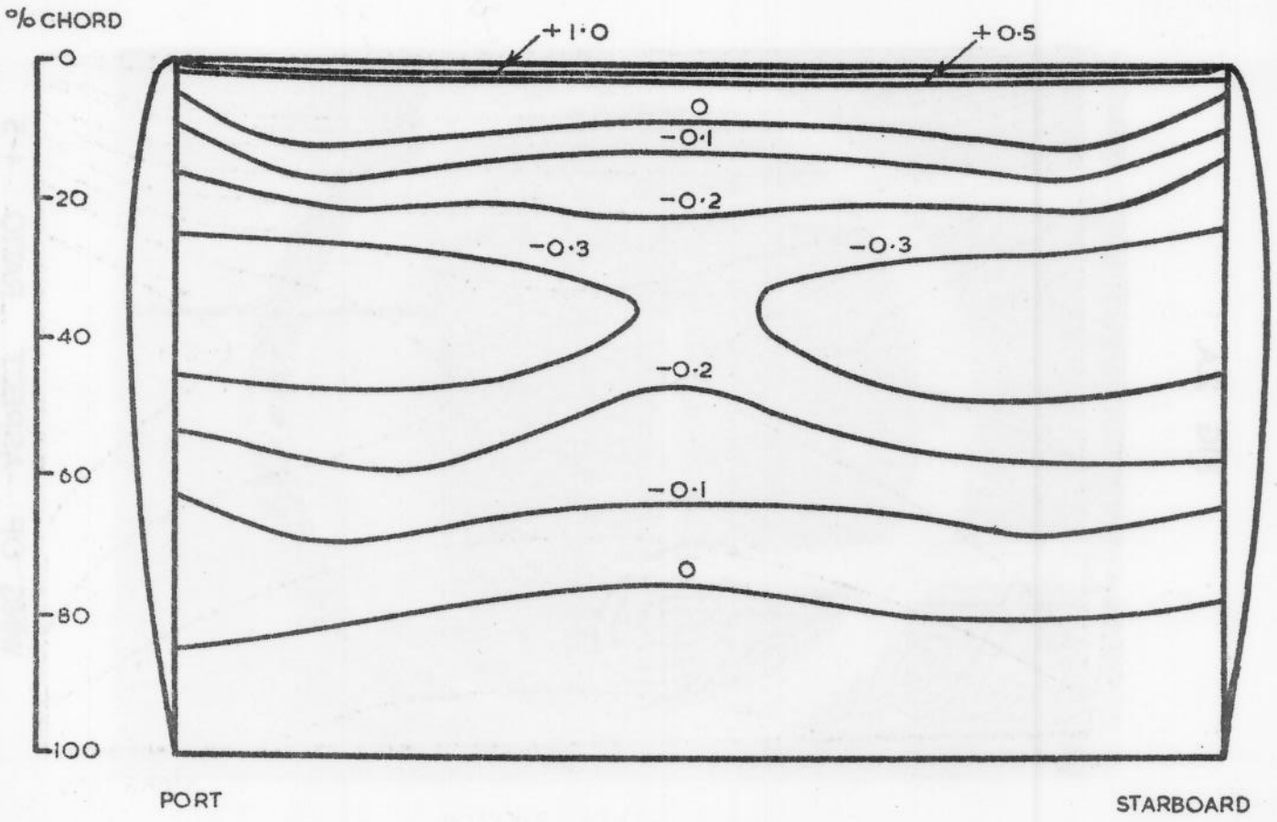

LOWER SURFACE

C_{NF} (OVERALL) = 0·17, $\Psi = 0°$

ISOBARS —— A.R. = 1·5.

COLLEGE OF AERONAUTICS

REPORT No. 52.

FIG. 4.

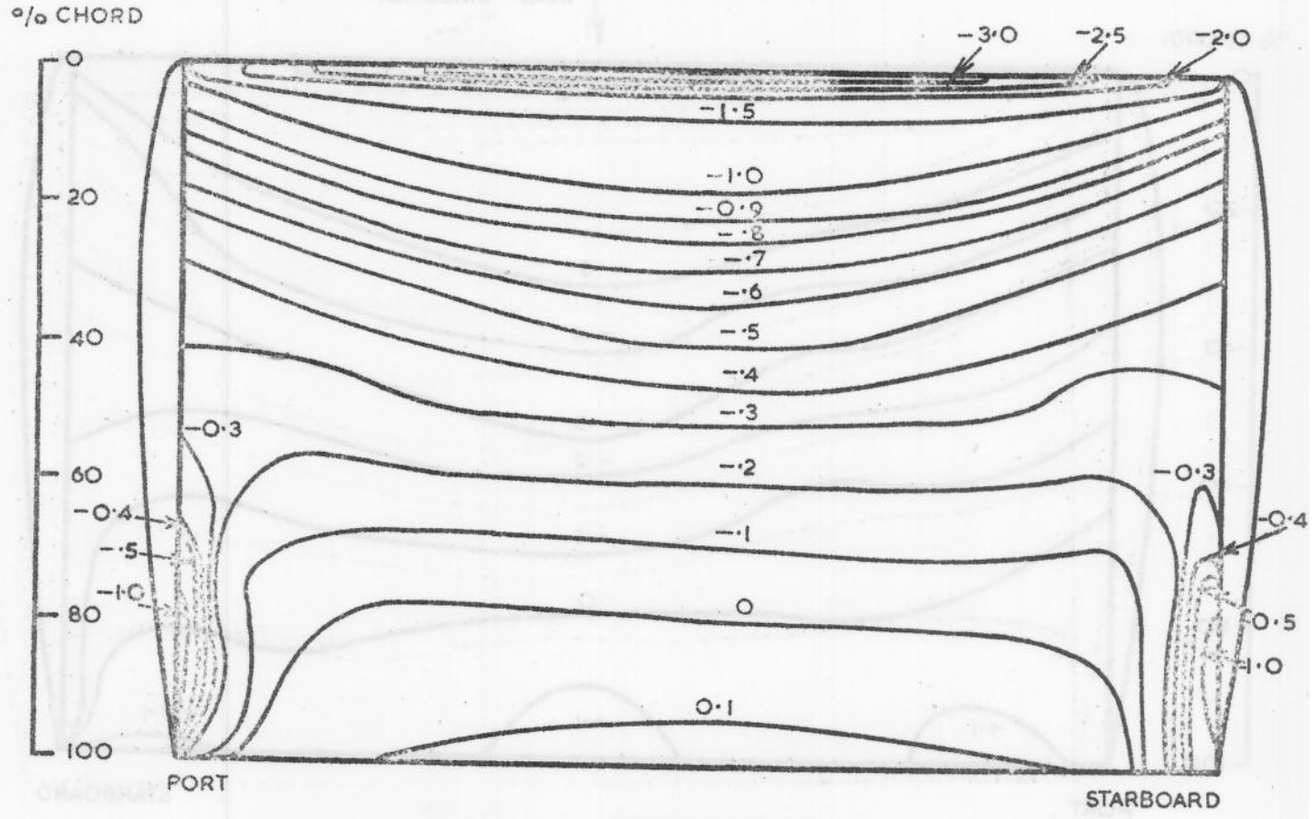

UPPER SURFACE

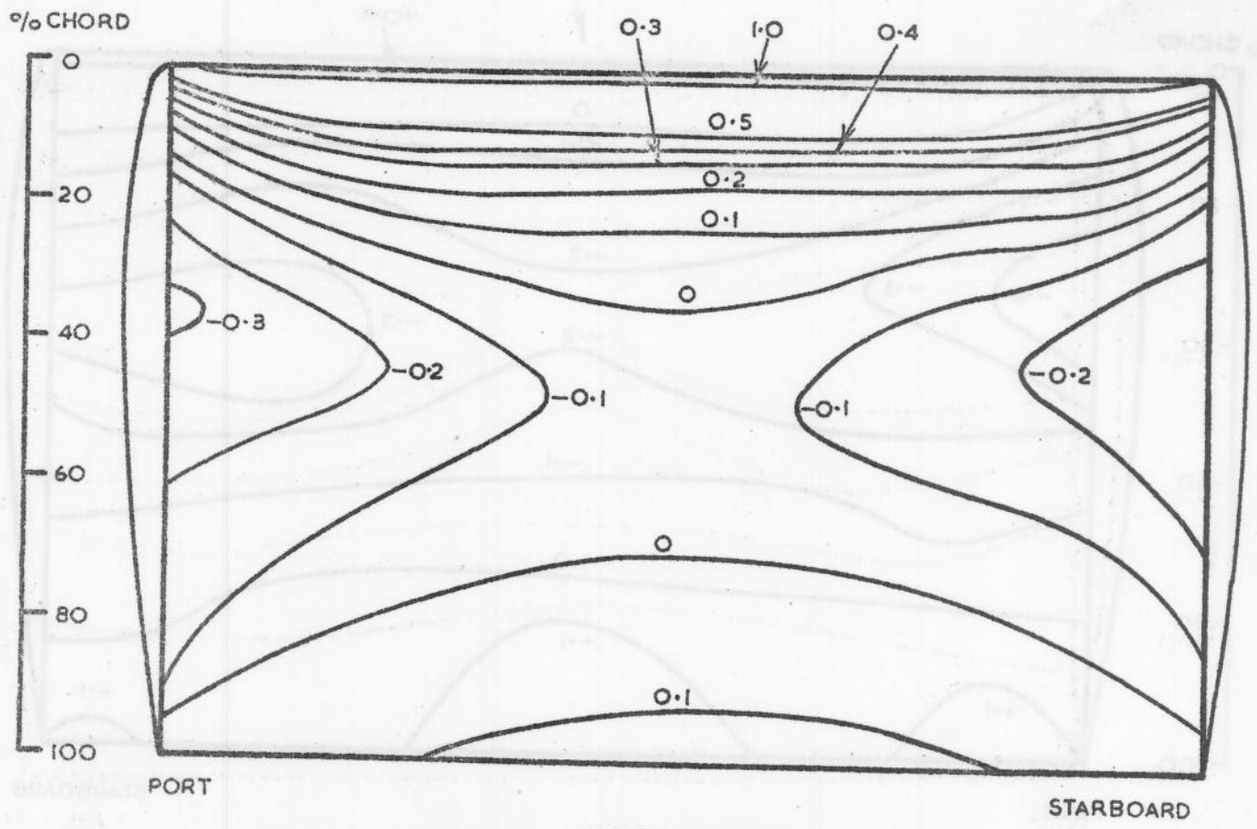

LOWER SURFACE.

C_{NF} (OVERALL) = 0·52, $\psi = 0°$

ISOBARS A. R. = 1·5

COLLEGE OF AERONAUTICS

REPORT No. 52.

FIG. 5.

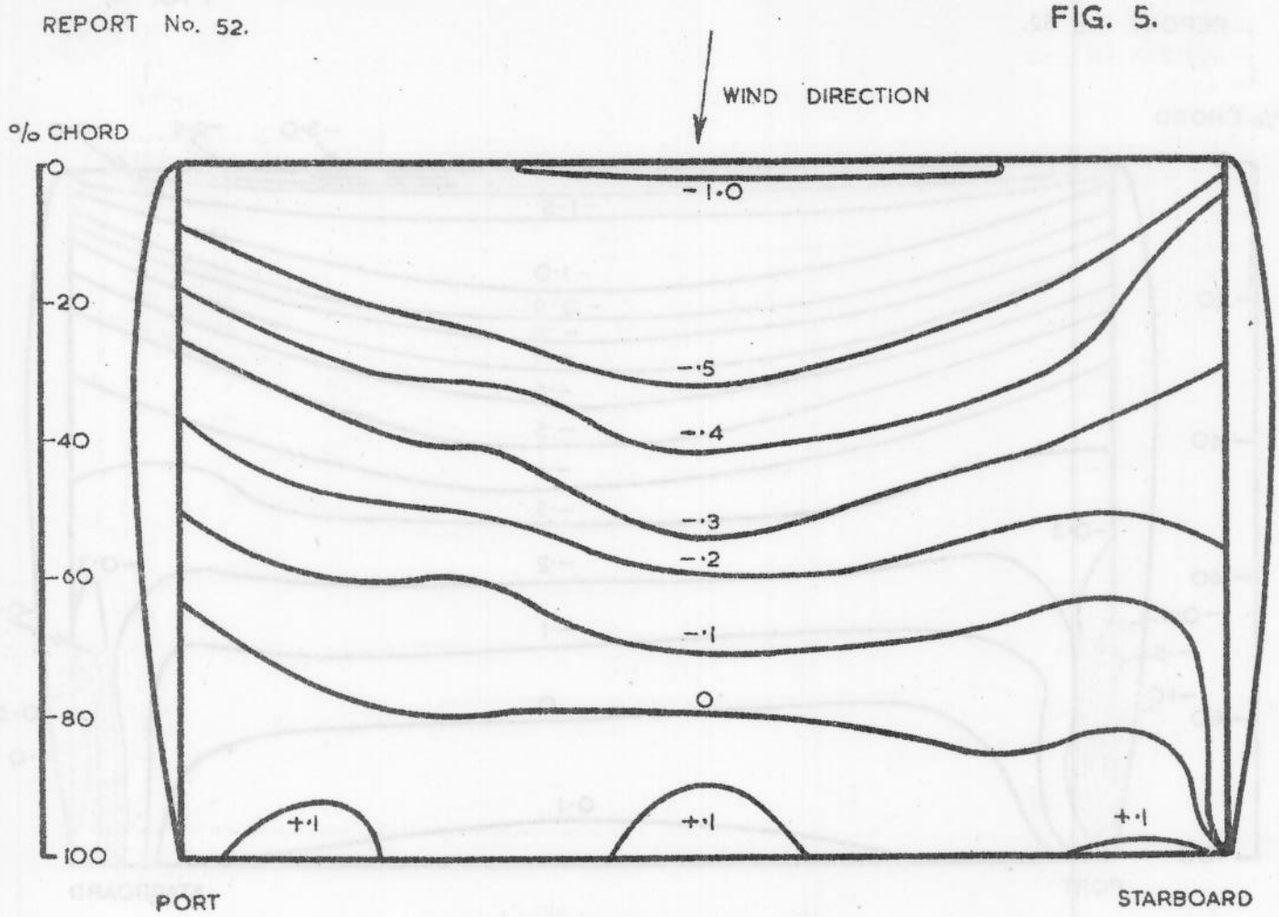

UPPER SURFACE

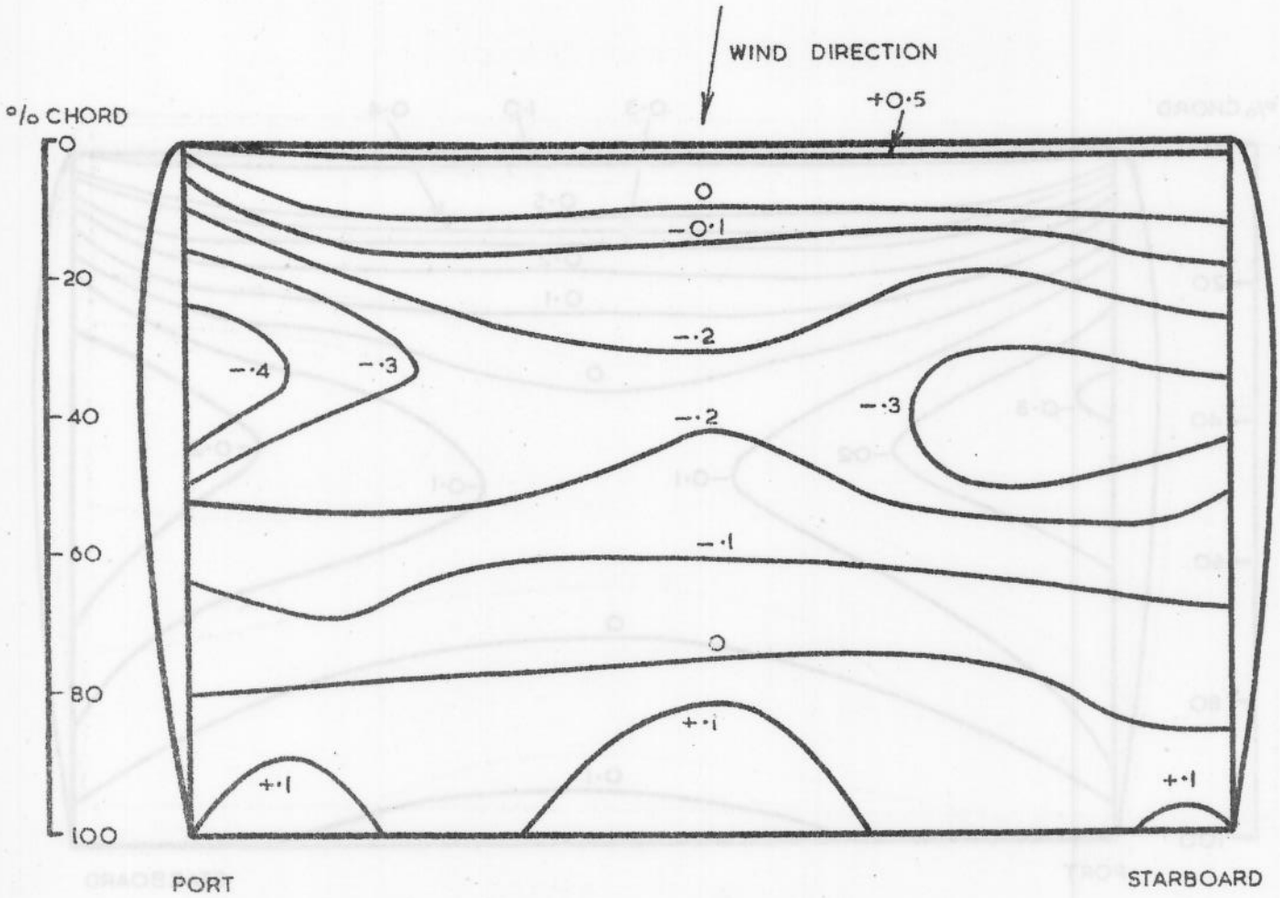

LOWER SURFACE

C_{NF} (OVERALL AT $\psi = 0°$) = 0·17, $\psi = 10°$

ISOBARS — A.R. = 1·5.

COLLEGE OF AERONAUTICS

REPORT No. 52.

FIG. 6.

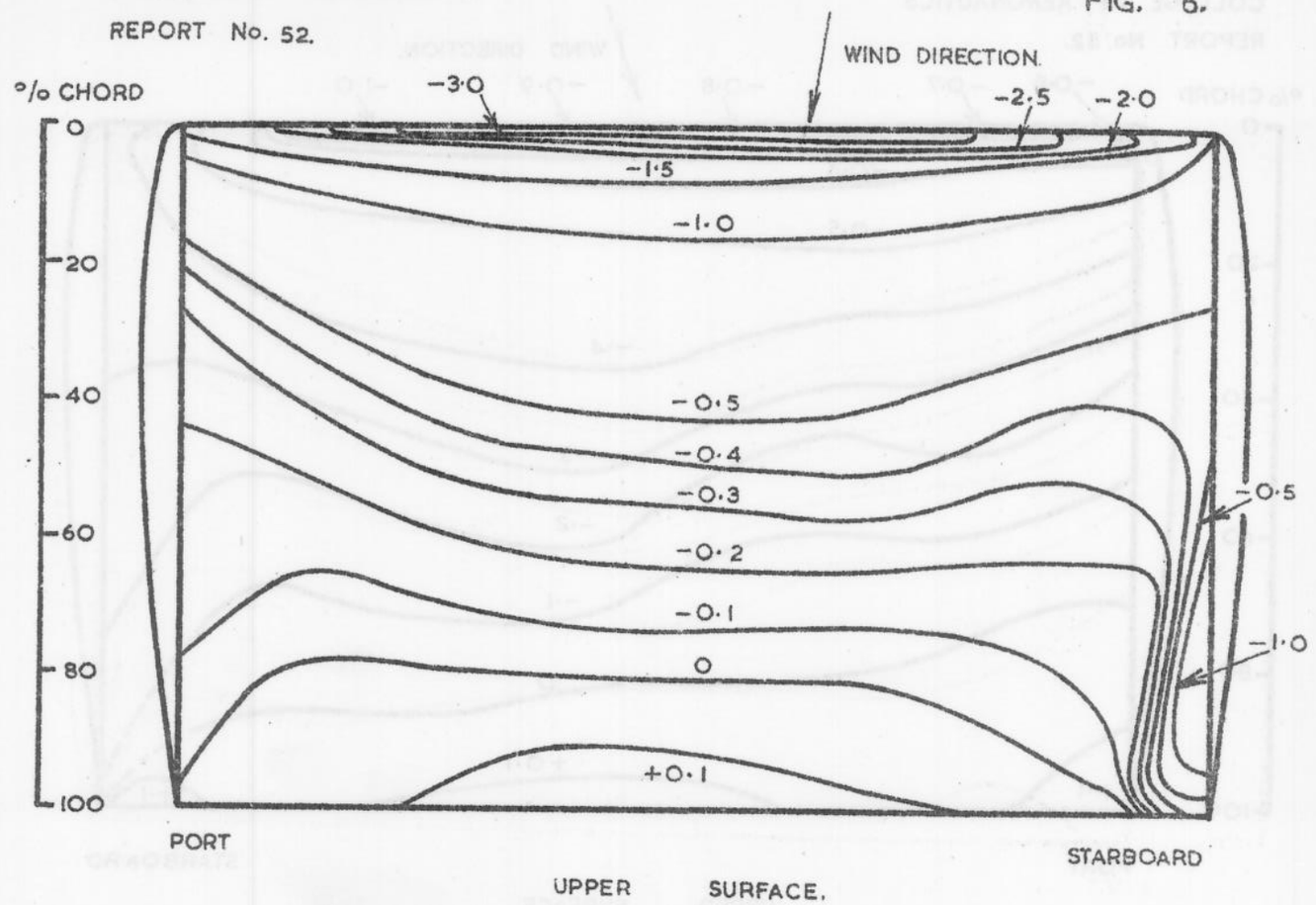

UPPER SURFACE.

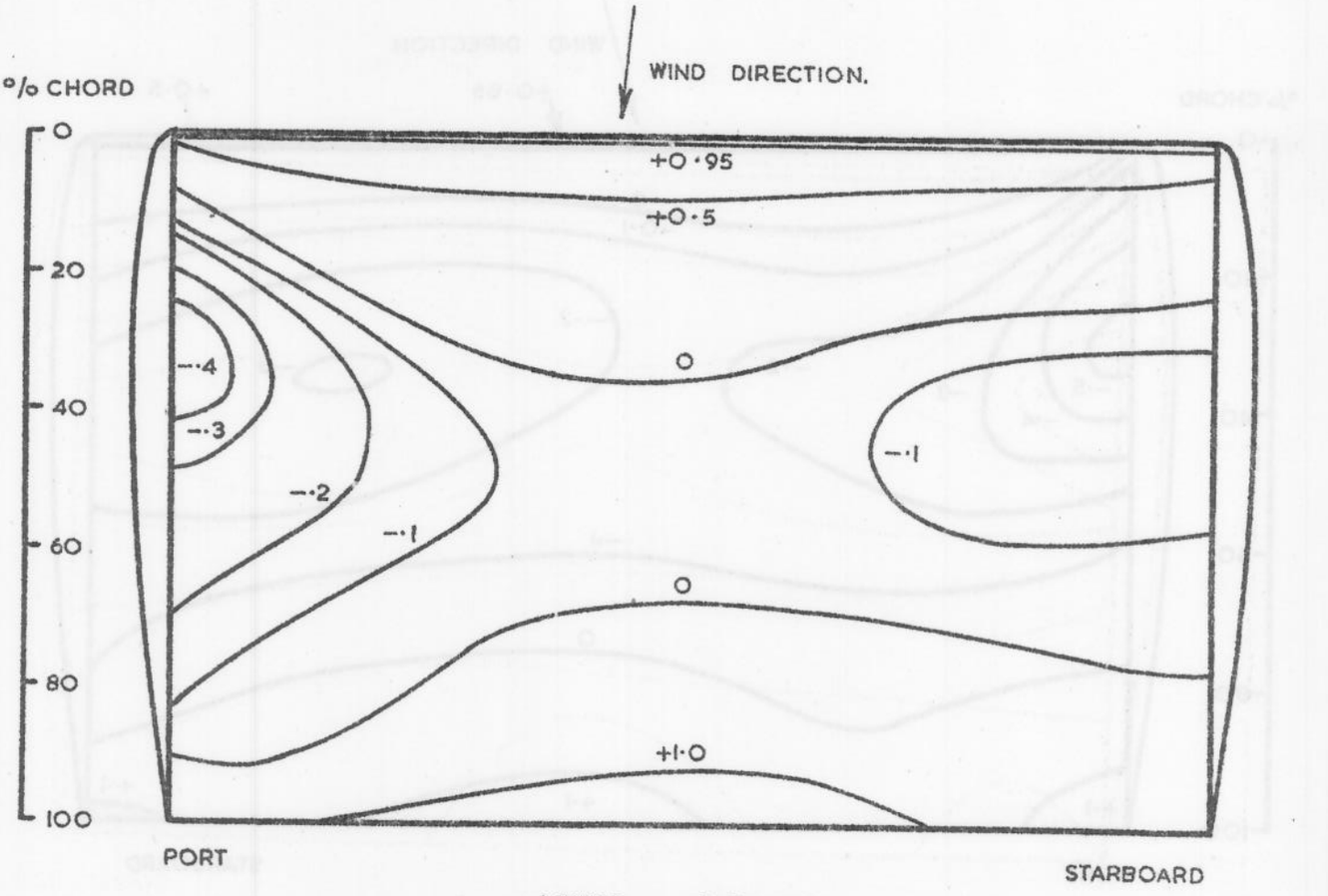

LOWER SURFACE.

C_{NF} (OVERALL AT $\psi = 0°$) $= 0.52, \psi = 10°$

ISOBARS. —— A.R. = 1·5

COLLEGE OF AERONAUTICS

REPORT No. 52.

FIG. 7.

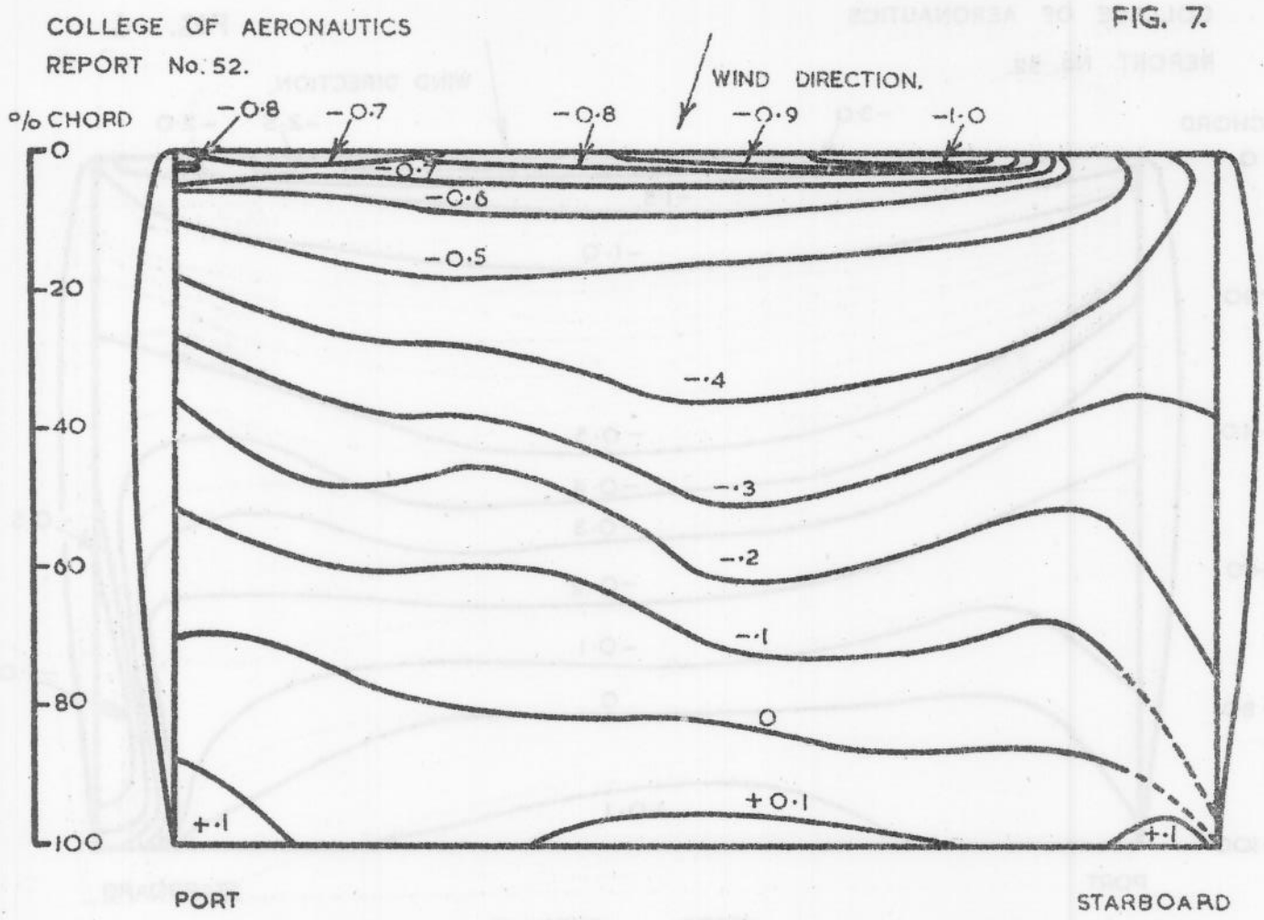

UPPER SURFACE

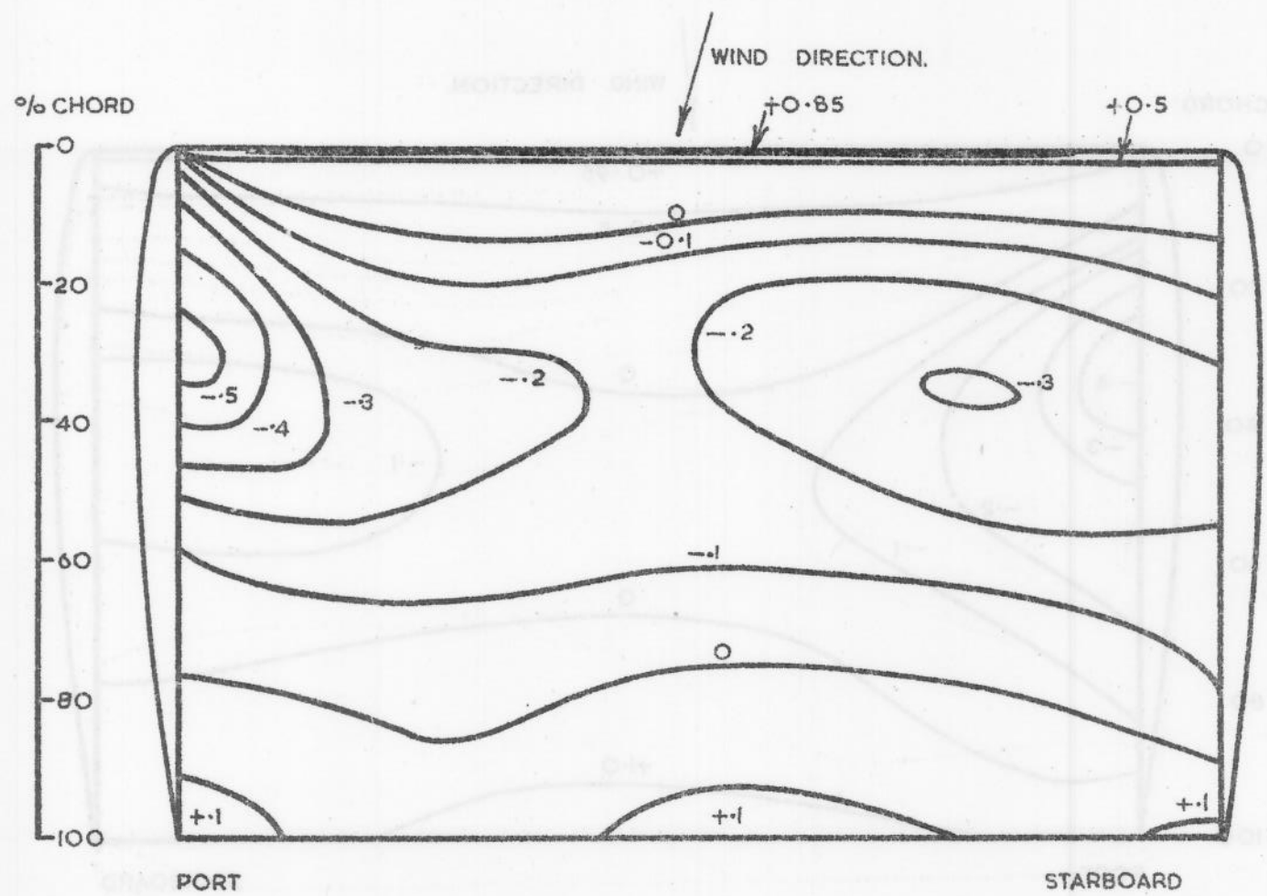

LOWER SURFACE

C_{NF} (OVERALL $\psi = 0°$) = 0·17, ψ = 20°

ISOBARS —— A.R. = 1·5

COLLEGE OF AERONAUTICS

REPORT No. 52.

FIG. 8.

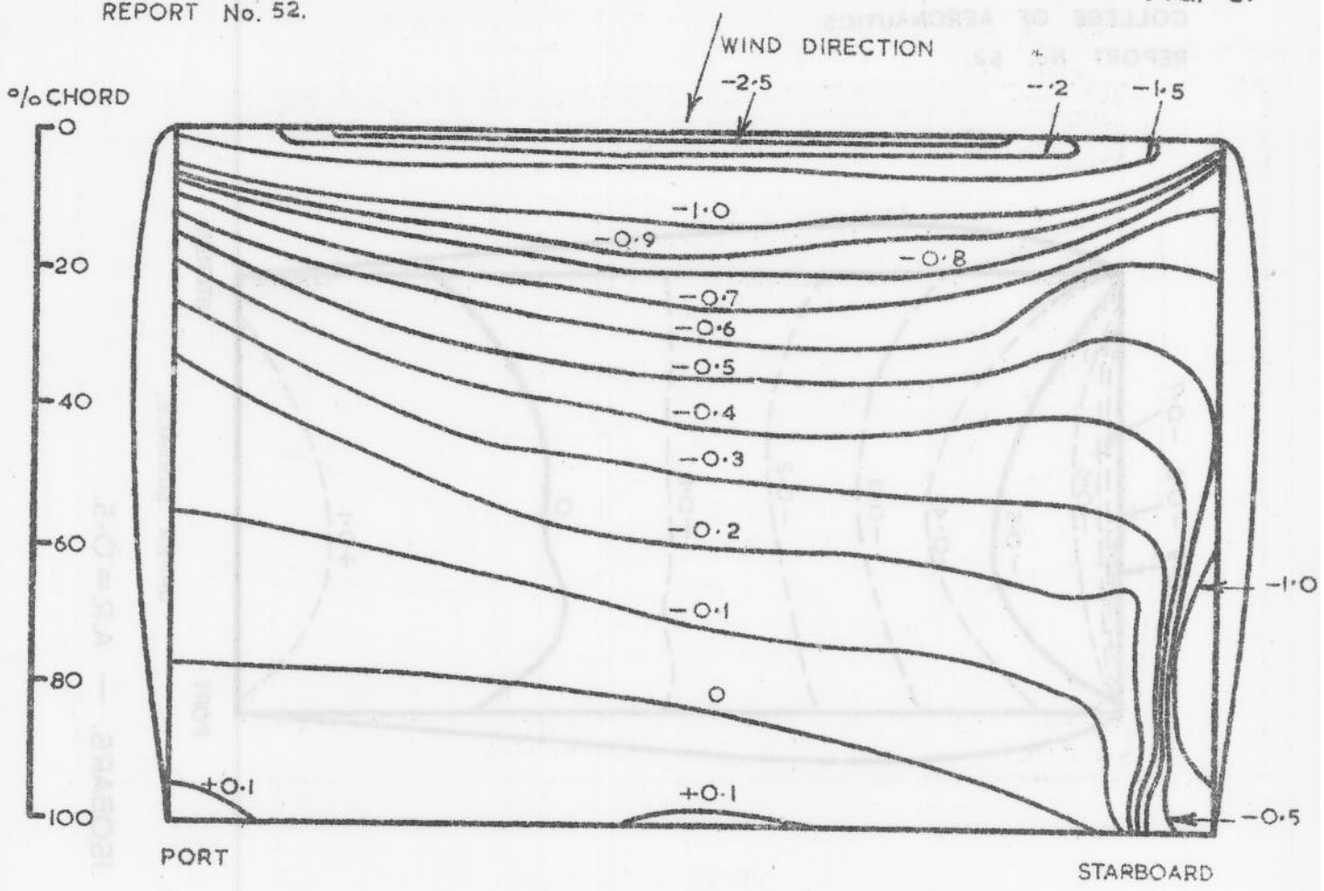

UPPER SURFACE.

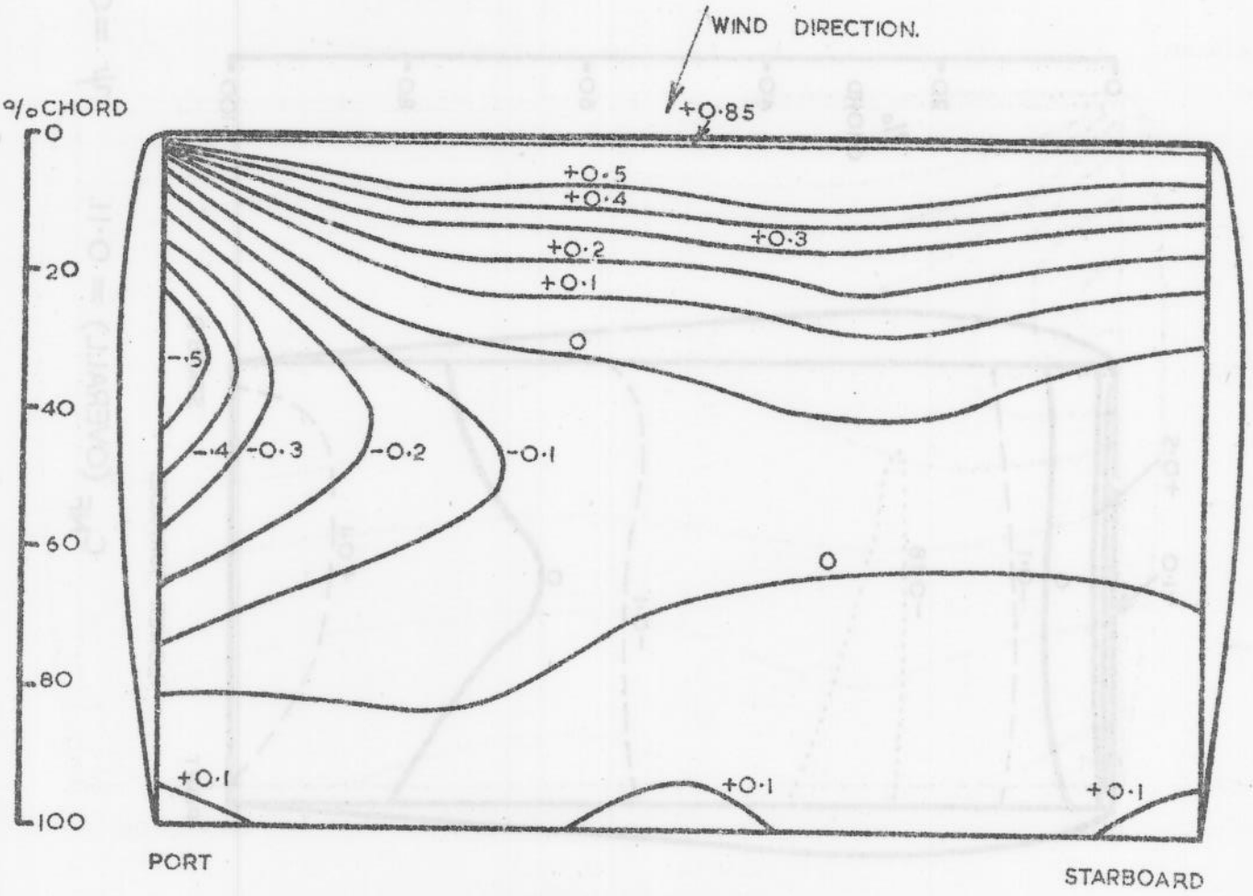

LOWER SURFACE.

C_{NF} (OVERALL AT $\psi = 0$) = 0·52, $\psi = 20°$

ISOBARS — A.R. = 1·5

FIG. 9.

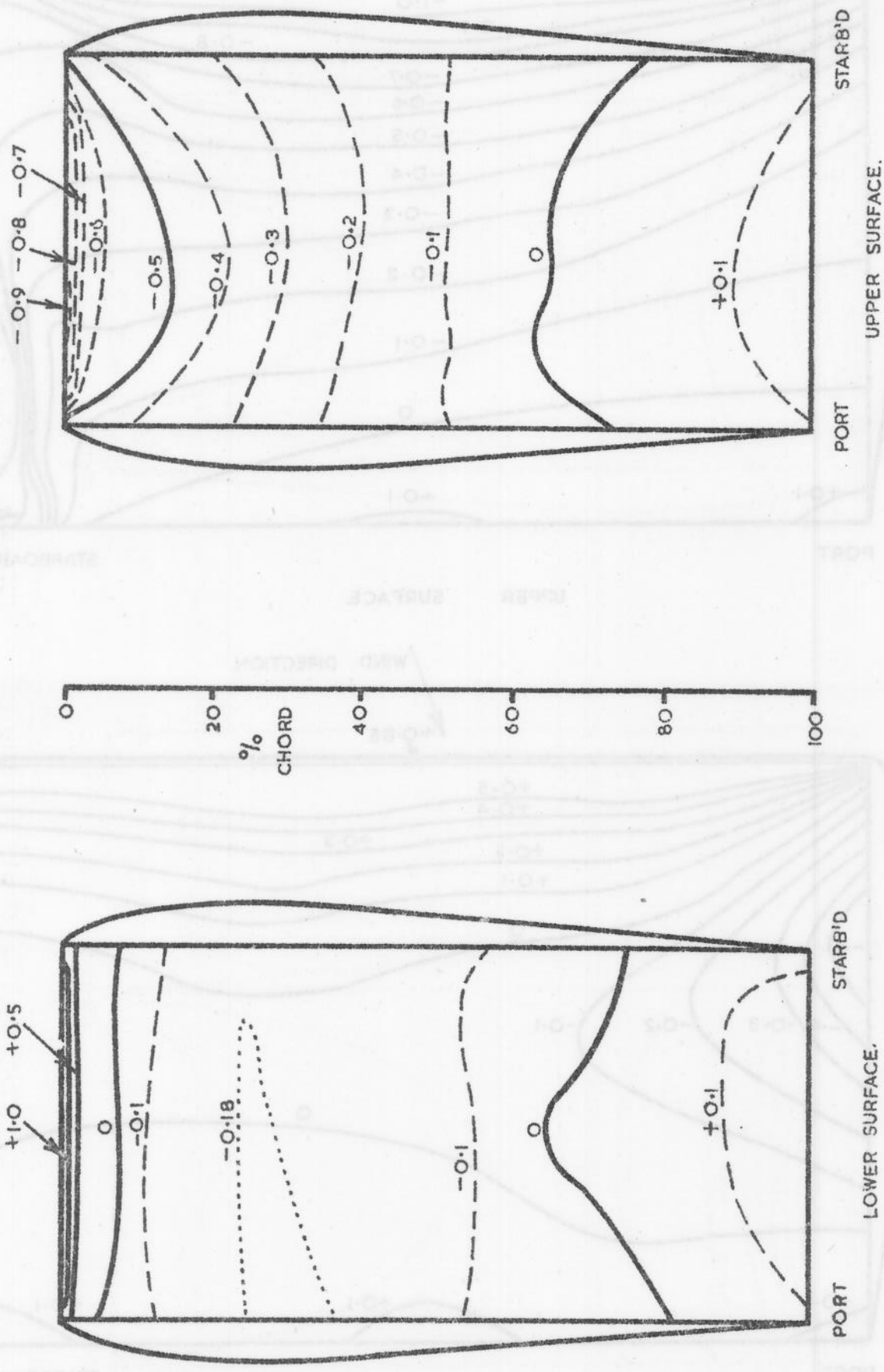

C_{NF} (OVERALL) = 0·11. $\psi = 0^{\circ}$ ISOBARS. — A.R. = 0·5.

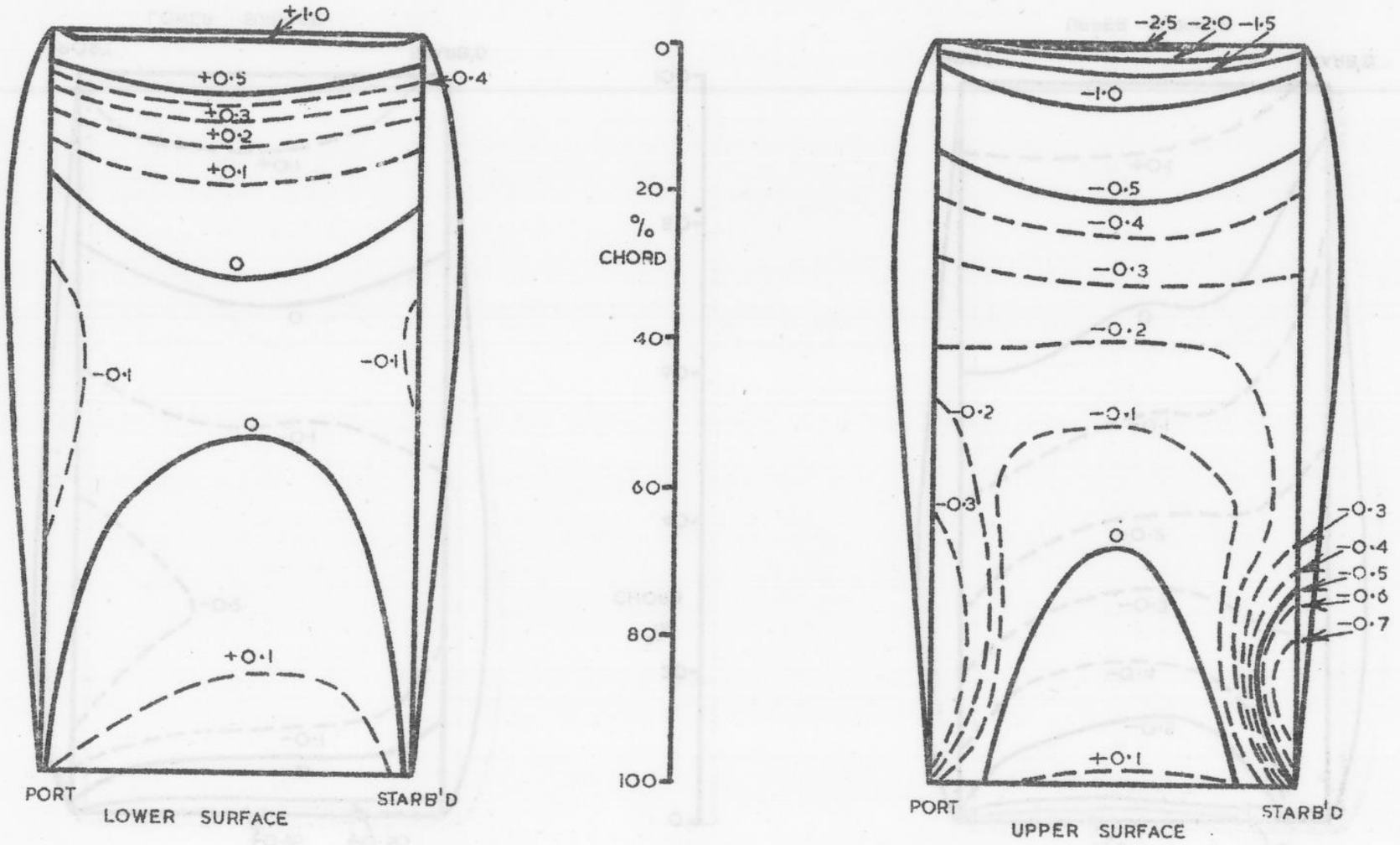

C_{NF}(OVERALL) = 0·41 $\psi = 0^{\circ}$ ISOBARS — A.R. = 0·5.

COLLEGE OF AERONAUTICS
REPORT No. 52.

FIG 10

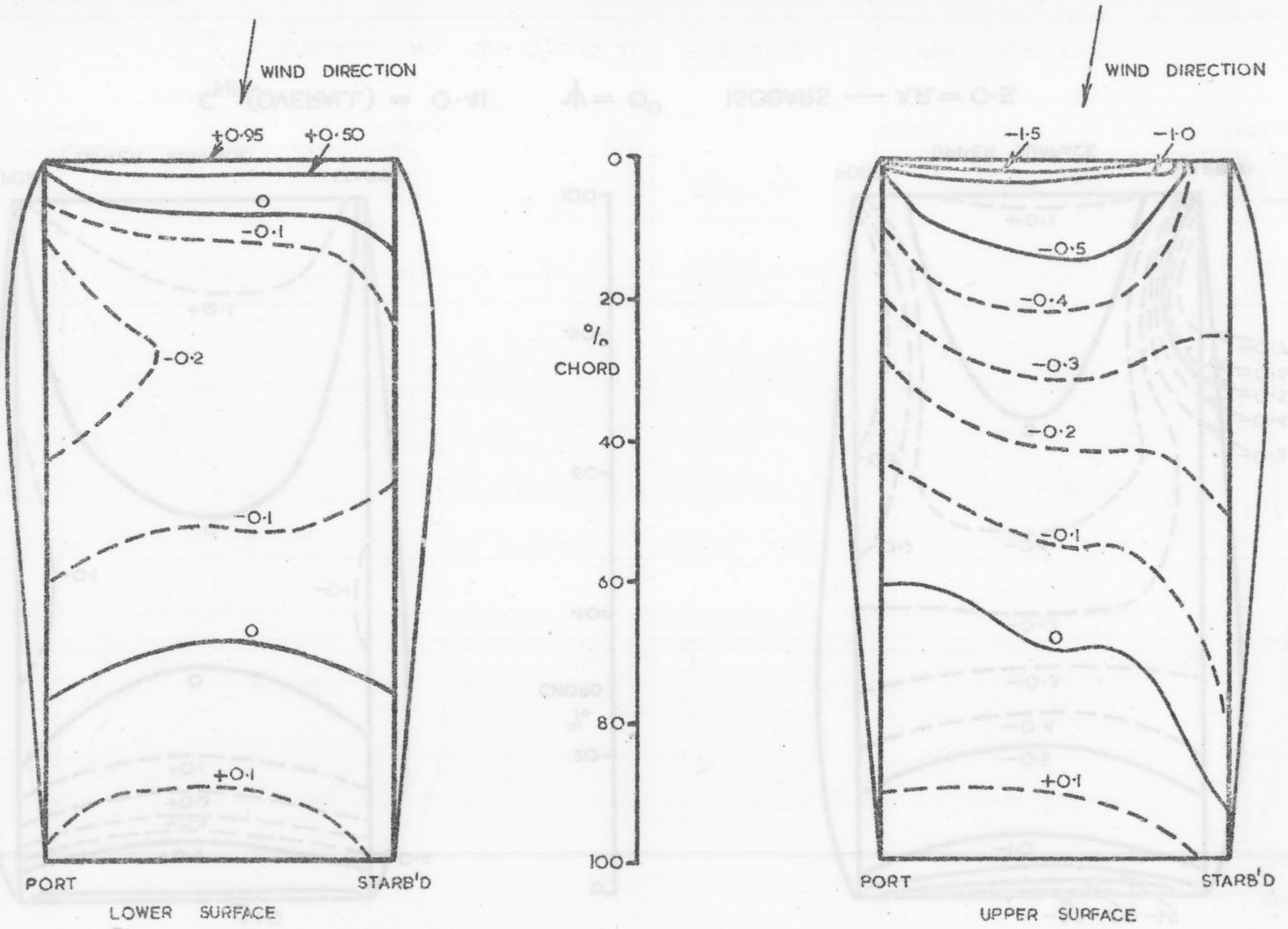

C_{NF} (OVERALL AT $\psi = 0°$) = 0·11 $\psi = 10°$ ISOBARS — A.R. = 0·5.

COLLEGE OF AERONAUTICS
REPORT No. 52.

FIG. 11.

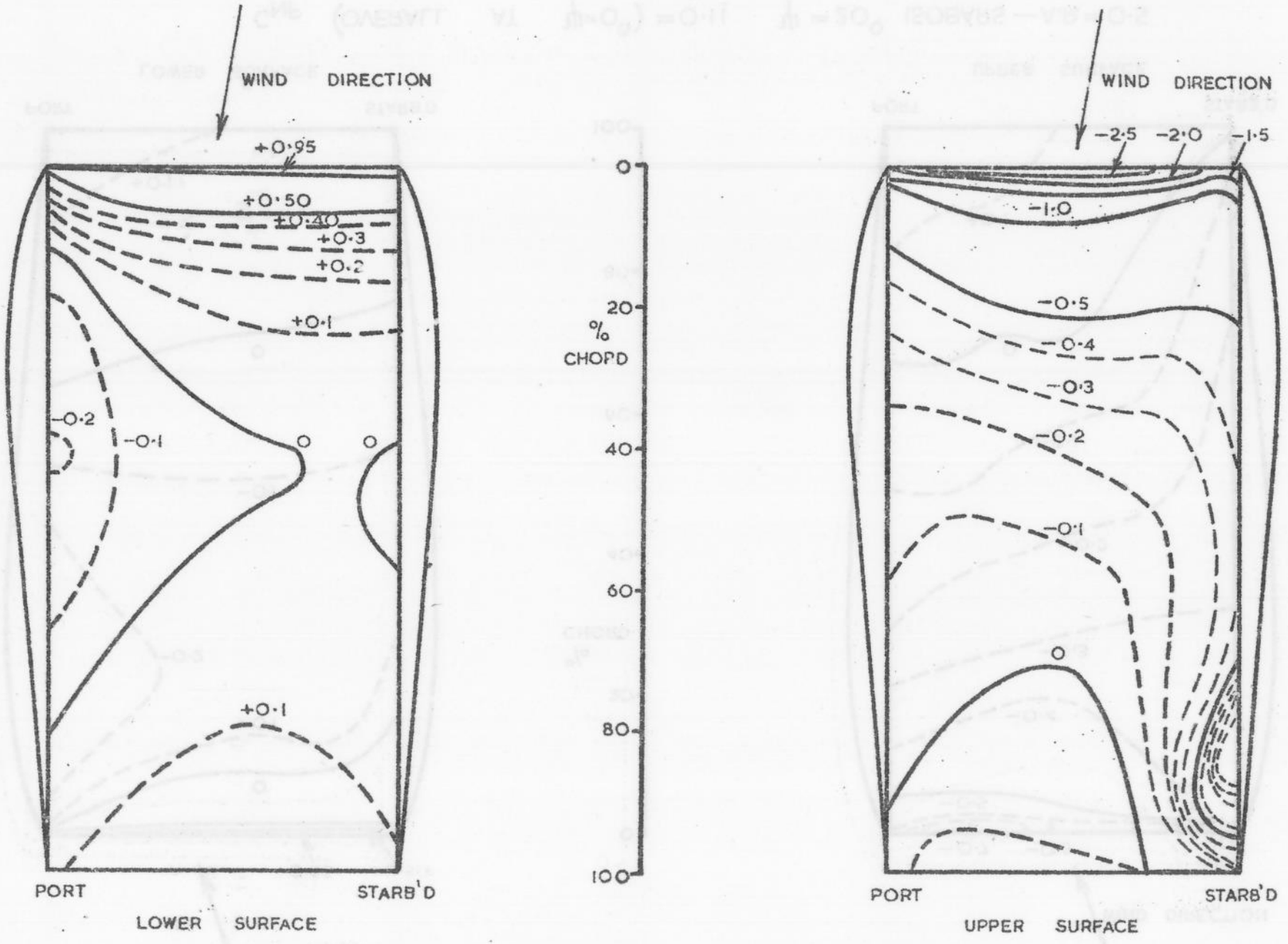

C_{NF} (OVERALL AT $\psi = 0$) = 0·41. $\psi = 10°$ ISOBARS — A.R. = 0·5.

COLLEGE OF AERONAUTICS
REPORT No. 52.

FIG 12

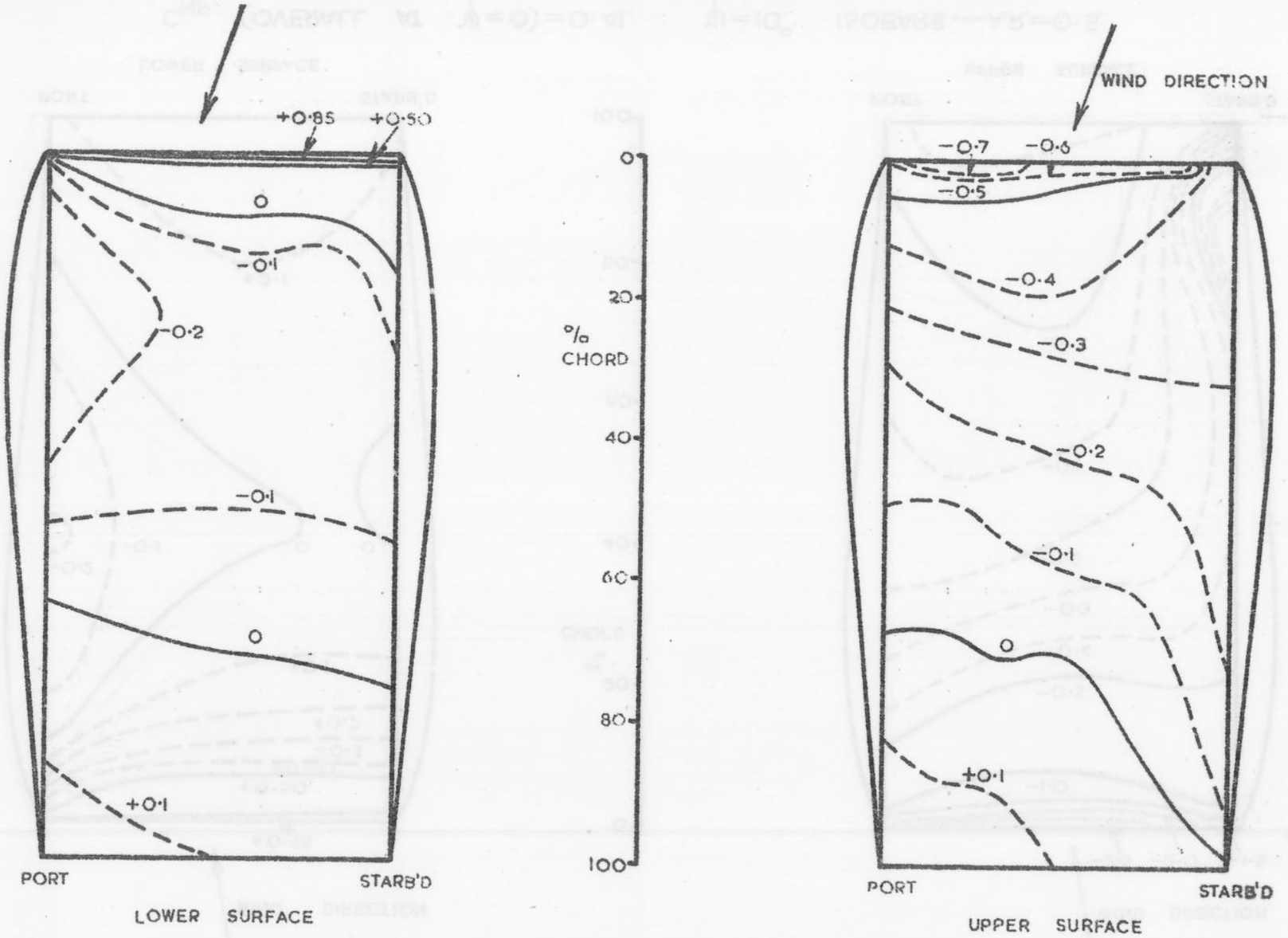

C_{NF} (OVERALL AT $\psi=0^{\circ}$) $=0\cdot11$ $\psi=20^{\circ}$ ISOBARS — A.R. $=0\cdot5$

COLLEGE OF AERONAUTICS
REPORT No. 52.

FIG. 13.

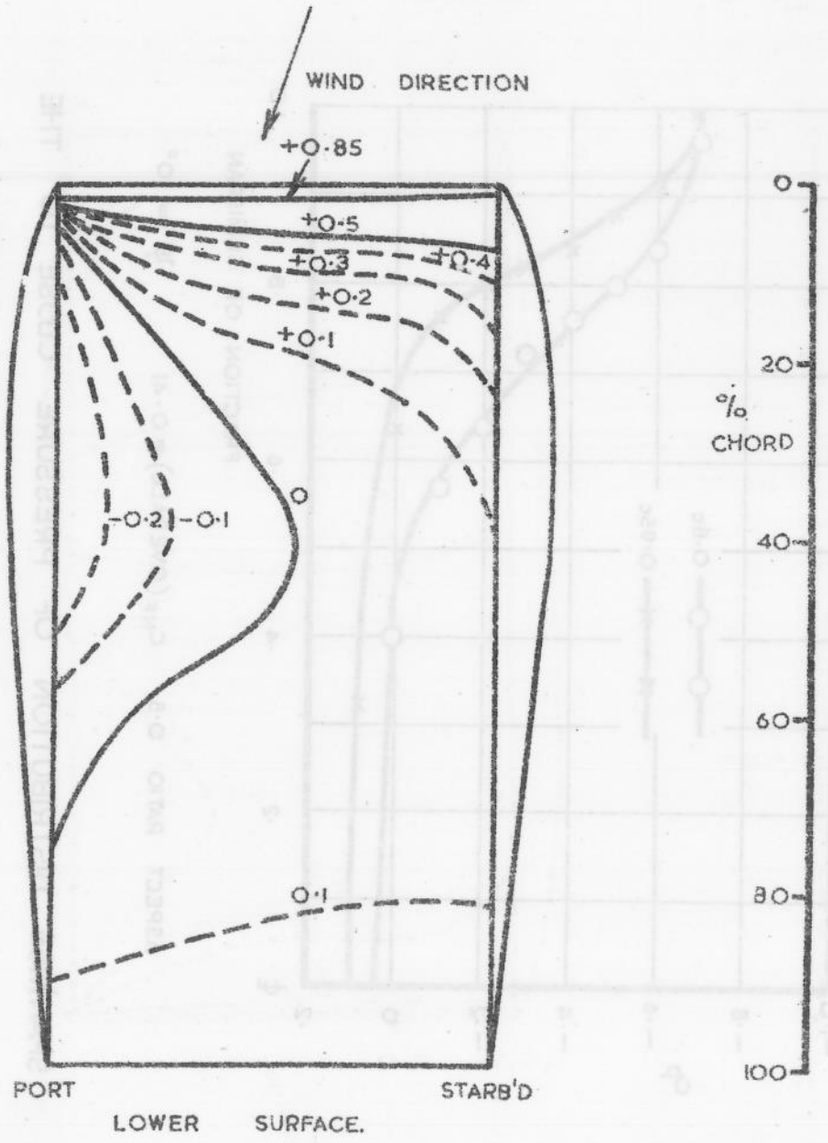

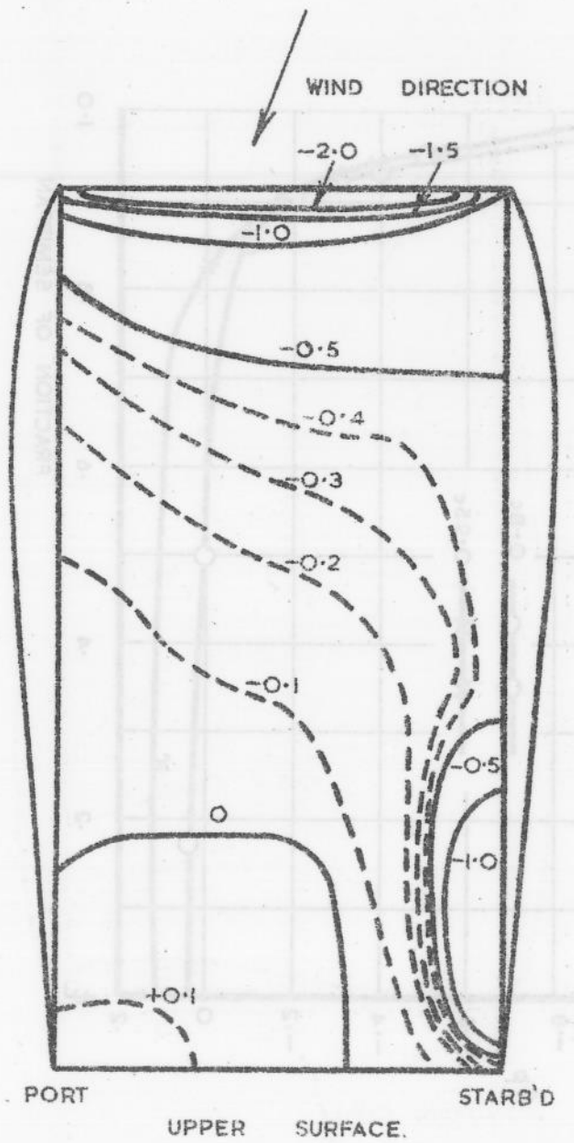

C_{NF} (OVERALL AT $\psi = 0°$) = 0·41 ψ = 20° ISOBARS — A.R. = 0·5.

COLLEGE OF AERONAUTICS
REPORT No. 52.

FIG. 14.

FIG 15.

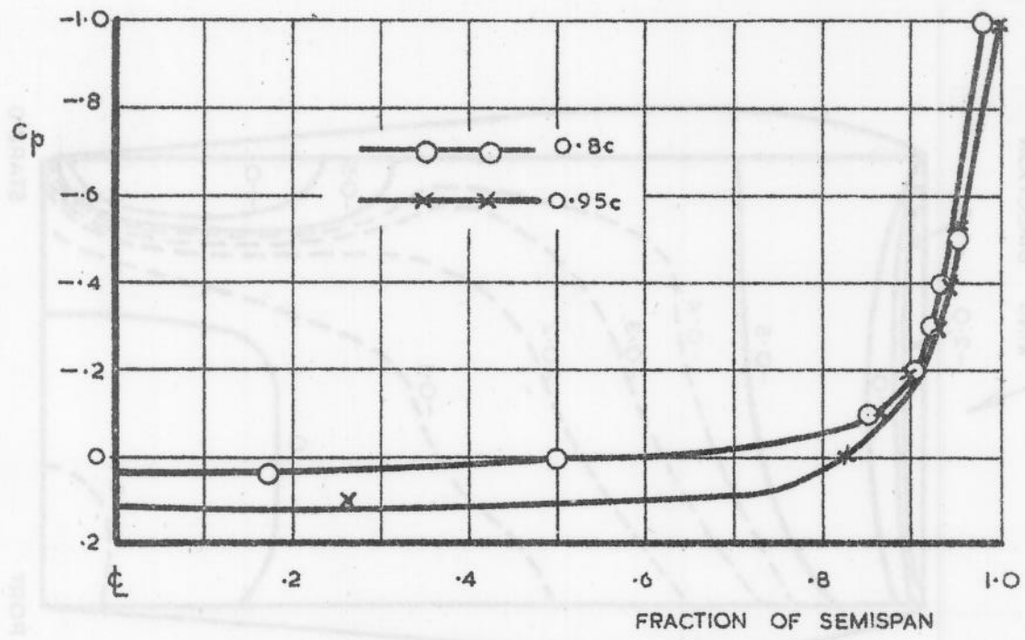

ASPECT RATIO 1·5 C_{NF} (OVERALL) = 0·52 $\psi = 0°$

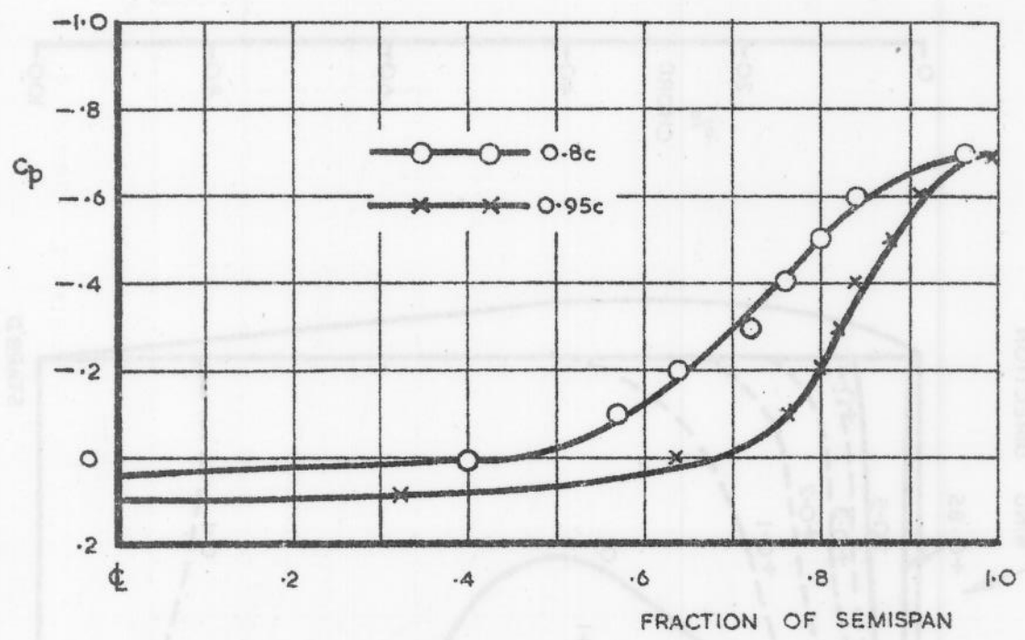

ASPECT RATIO 0·5 C_{NF} (OVERALL) = 0·41 $\psi = 0°$

SPANWISE DISTRIBUTION OF PRESSURE CLOSE TO THE TRAILING EDGE ON THE UPPER SURFACE.

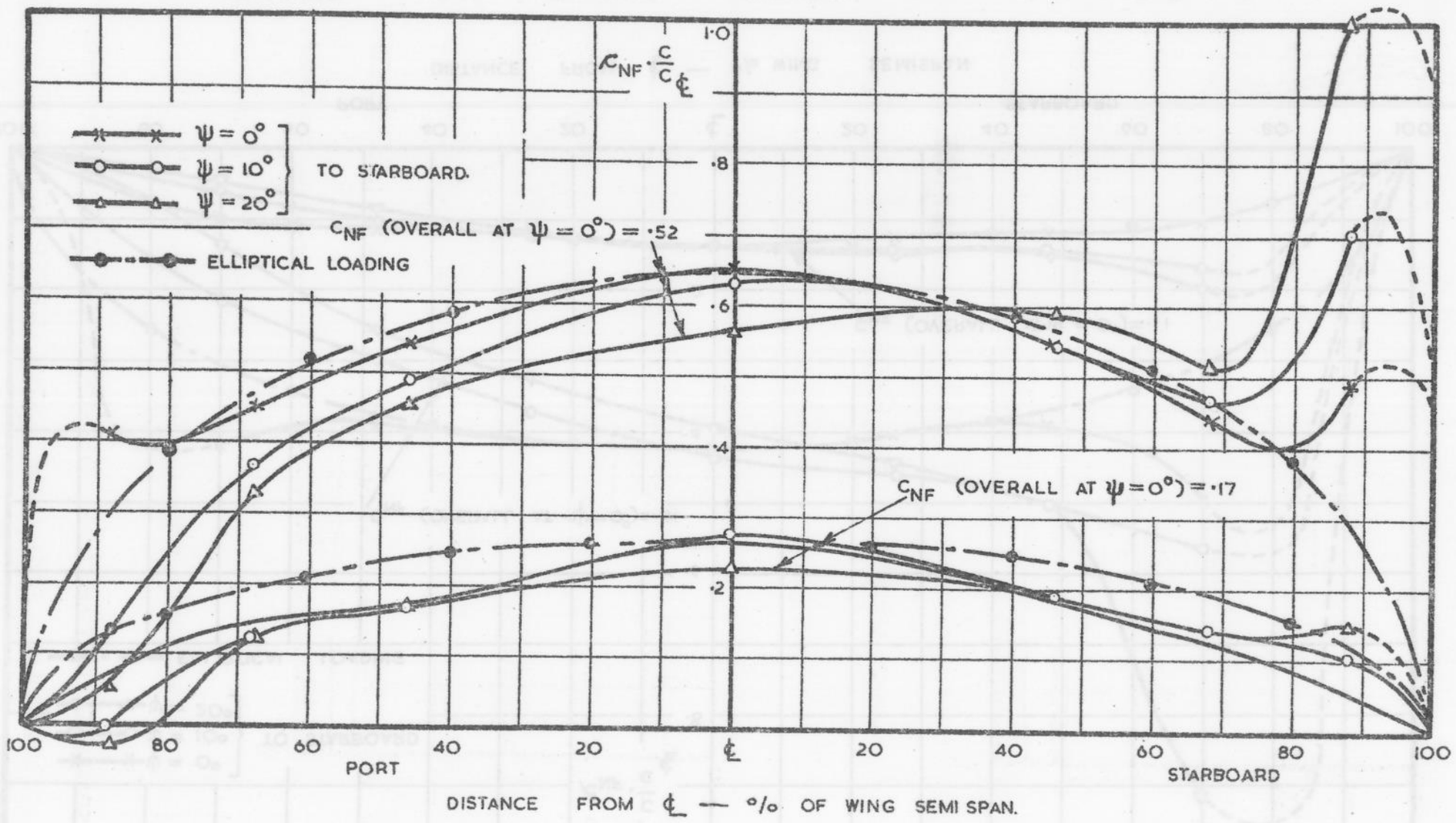

FIG. 16.

SPANWISE LOAD GRADING CURVES —— A.R. = 1·5

COLLEGE OF AERONAUTICS

REPORT No.

FIG. 17.

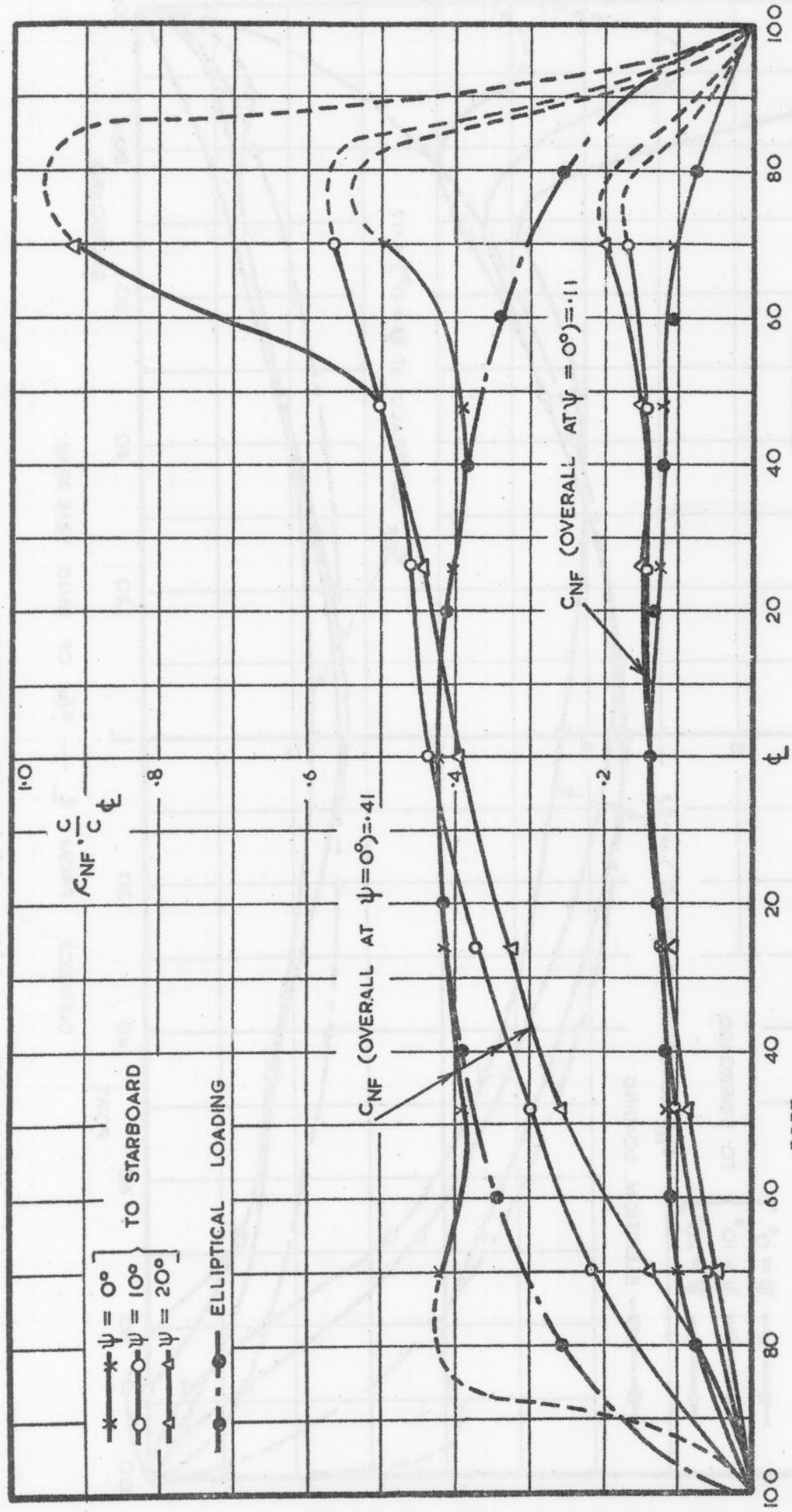

SPANWISE LOAD GRADING CURVES. —— A.R. = 0·5.

FIGS. 18A. & B.

FIG. 18.A.

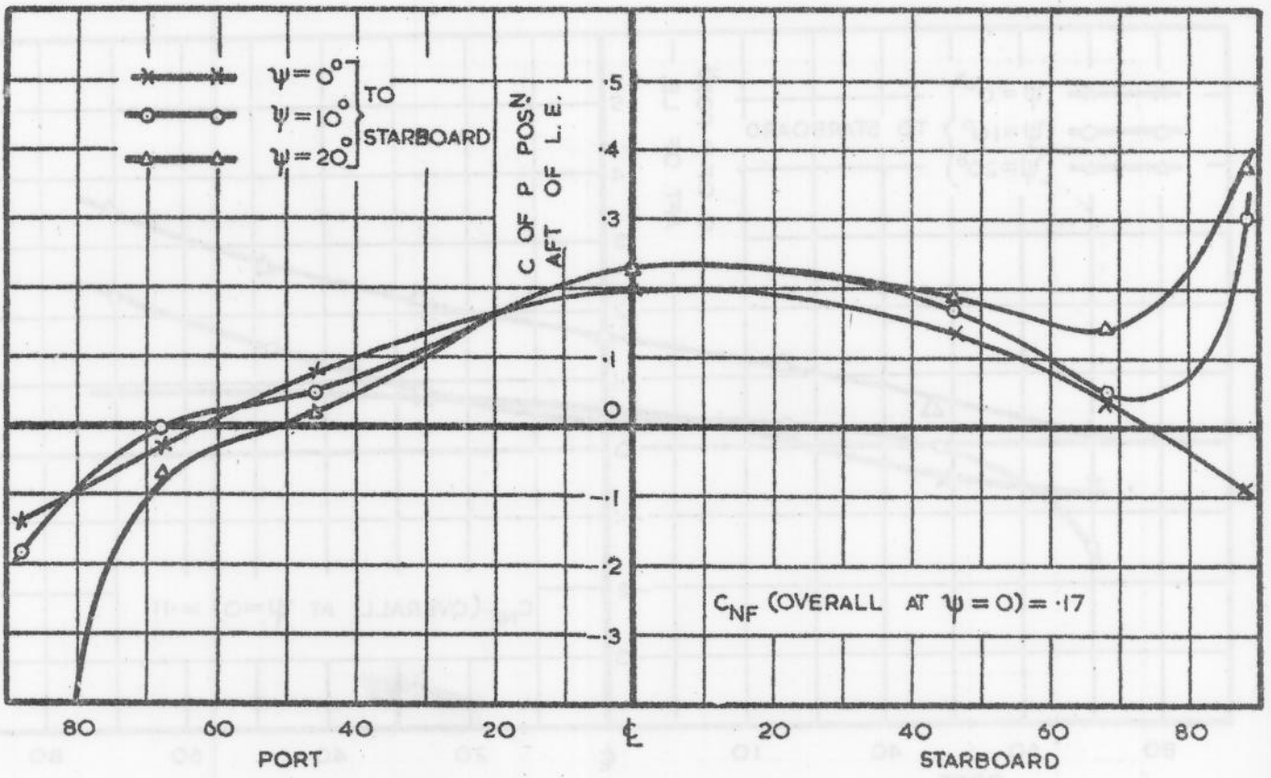

DISTANCE FROM ℄ — % OF WING SEMI-SPAN.

FIG. 18.B.

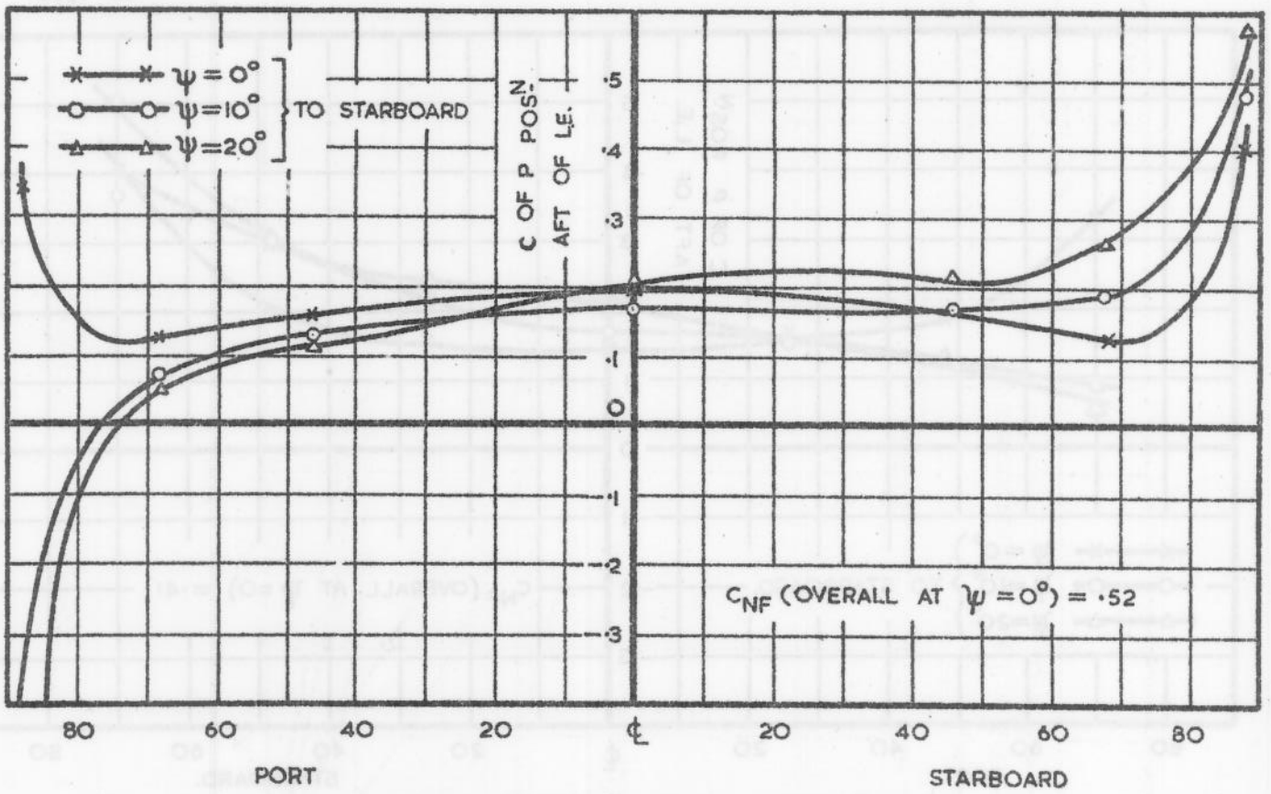

DISTANCE FROM ℄ — % OF WING SEMI-SPAN.

POSITION OF LOCAL CENTRE OF PRESSURE.

A.R. = 1·5.

FIGS. 19A. & B.

FIG. 19A.

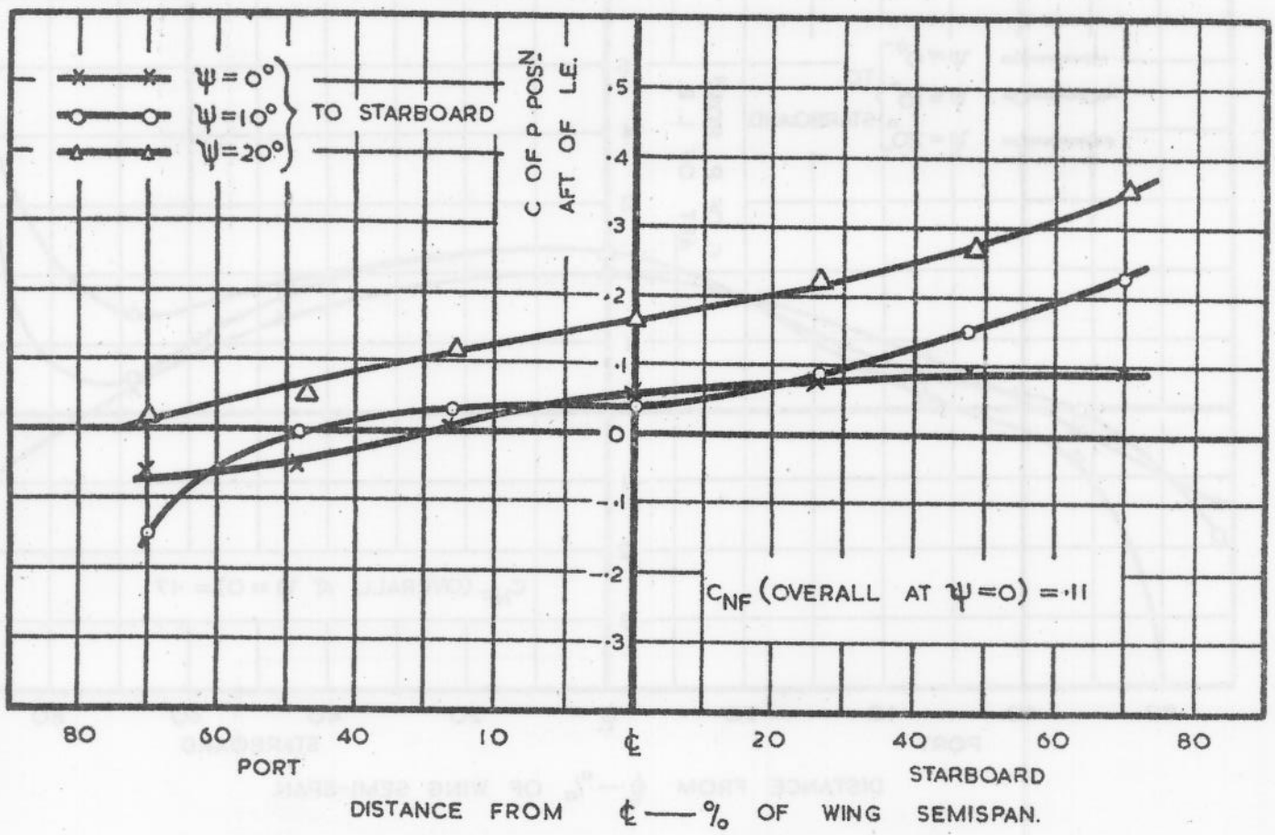

FIG. 19.B.

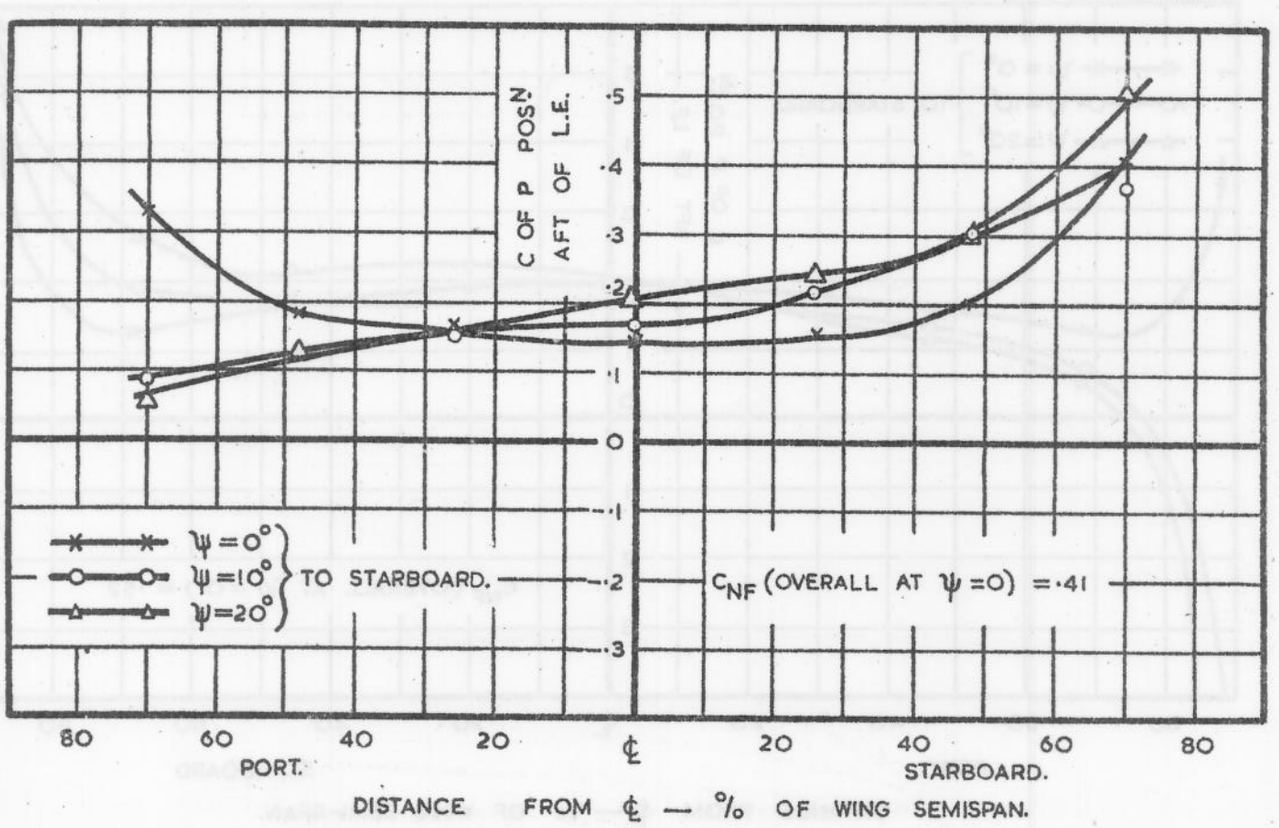

POSITION OF LOCAL CENTRE OF PRESSURE

A. R. = 0·5.

COLLEGE OF AERONAUTICS

REPORT No. 52.

FIGS. 20.A.B &C.

FIG. 20. A.

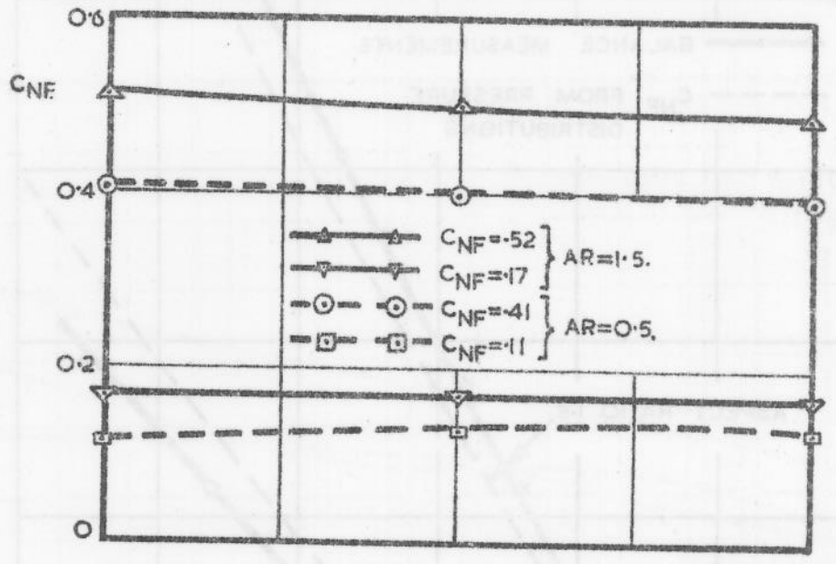

FIG. 20. B.

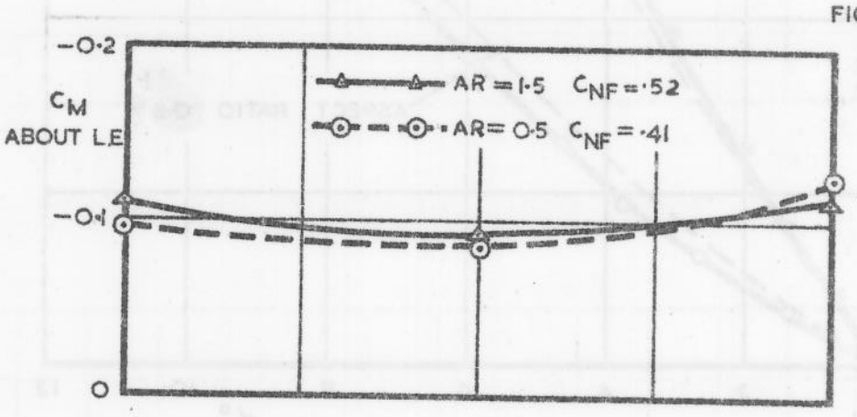

FIG. 20. C.

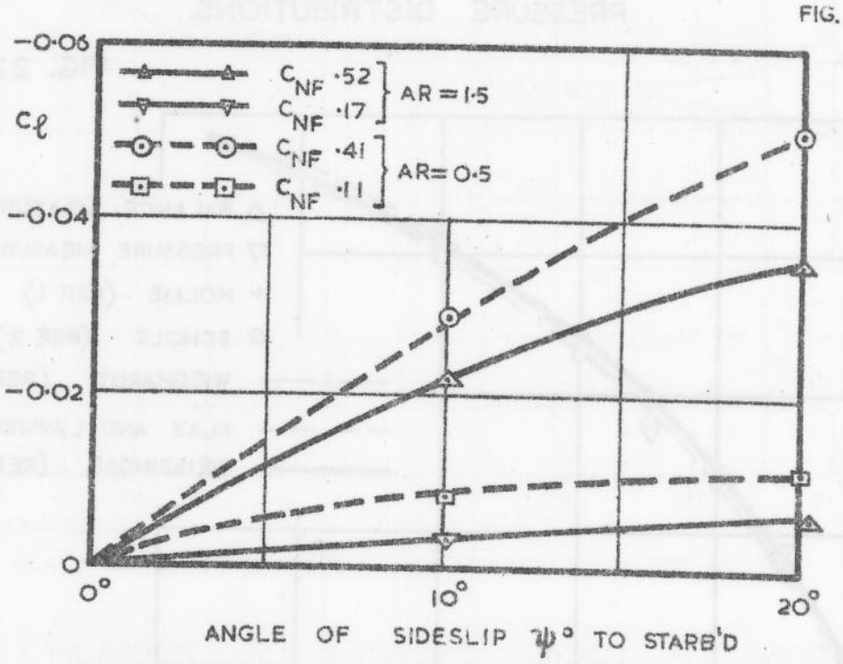

EFFECT OF SIDESLIP ON NORMAL FORCE, PITCHING AND ROLLING MOMENTS.

FIG. 21.

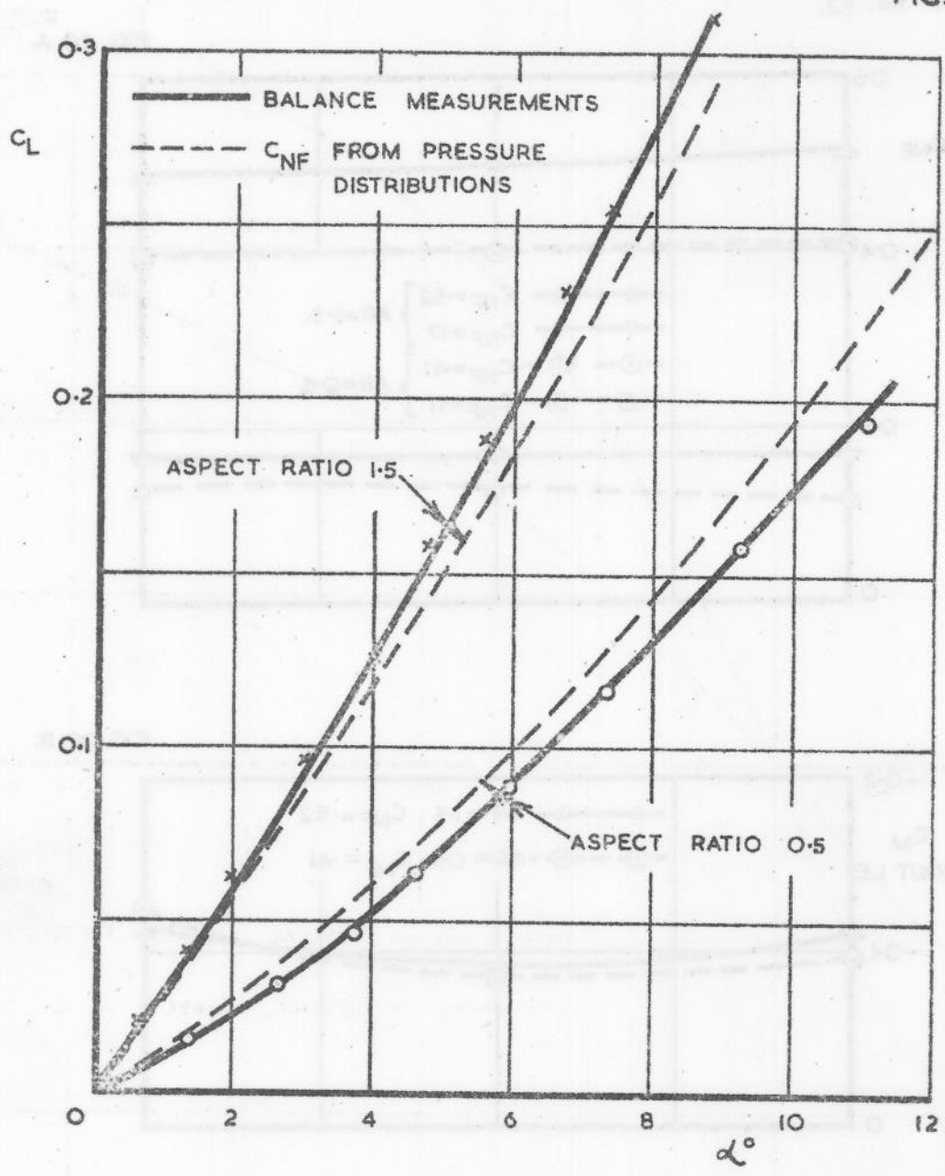

COMPARISON OF RESULTS FROM DIRECT MEASUREMENT AND PRESSURE DISTRIBUTIONS.

FIG. 22.

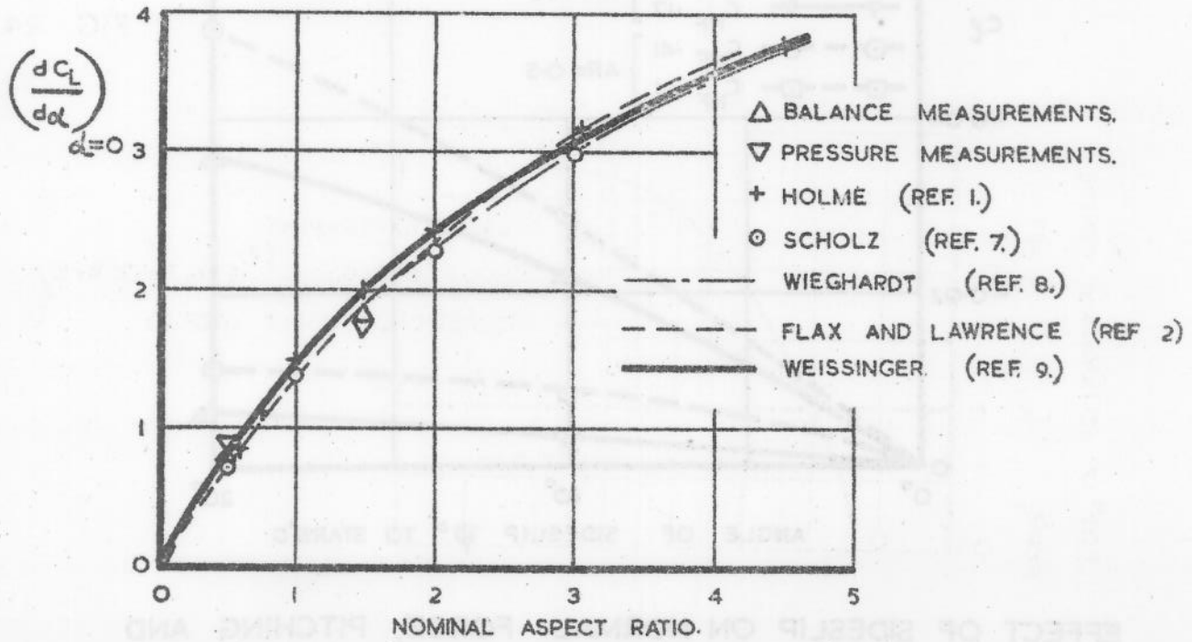

SLOPES OF LIFT CURVES.

COLLEGE OF AERONAUTICS

REPORT No. 52.

FIG. 23.

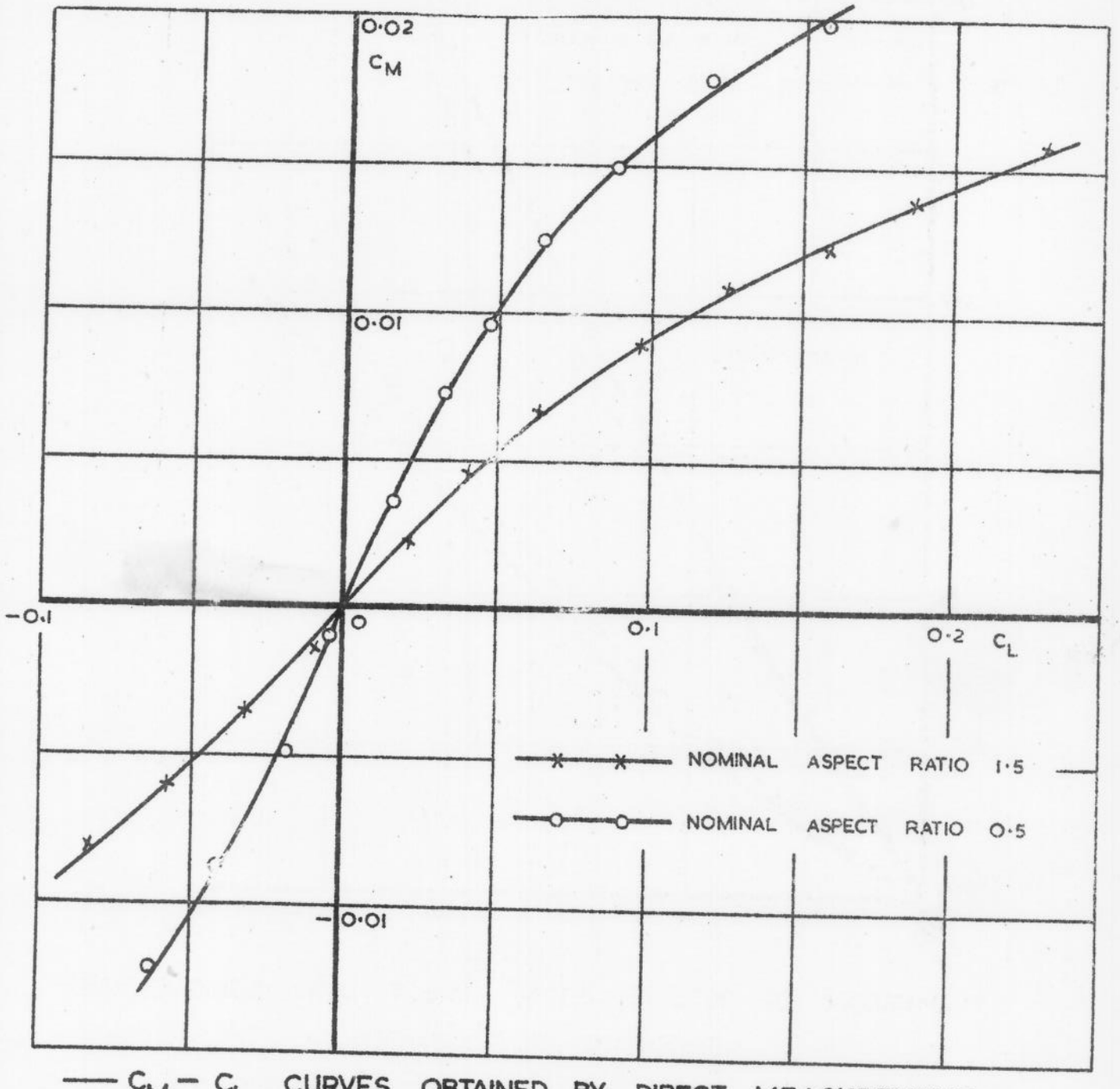

— $C_M - C_L$ CURVES OBTAINED BY DIRECT MEASUREMENT —

FIG. 24.

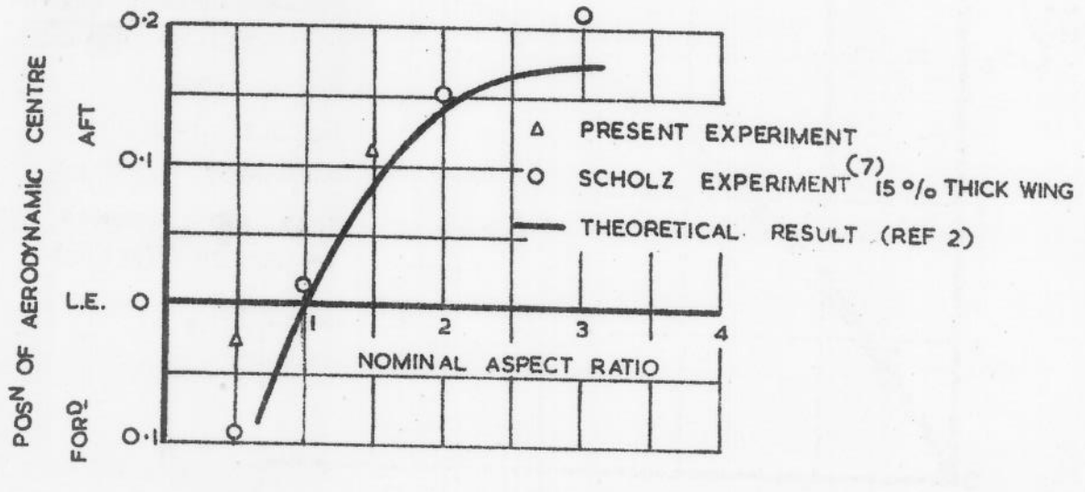

— COMPARISON WITH THEORETICAL RESULTS. —